Article

A Heuristic Approach for Determining Efficient Vaccination Plans under a SARS-CoV-2 Epidemic Model

Claudia Hazard-Valdés [1,*] and Elizabeth Montero [2,*]

1 Departamento de Informática, Universidad Técnica Federico Santa María, Santiago 8940000, Chile
2 Facultad de Ingeniería, Universidad Andres Bello, Viña del Mar 2531015, Chile
* Correspondence: claudia.hazard.14@sansano.usm.cl (C.H.-V.); elizabeth.montero@unab.cl (E.M.)

Abstract: In this work, we propose a local search-based strategy to determine high-quality allocation of vaccines under restricted budgets and time periods. For this, disease spread is modeled as a SEAIR pandemic model. Subgroups are used to understand and evaluate movement restrictions and their effect on interactions between geographical divisions. A tabu search heuristic method is used to determine the number of vaccines and the groups to allocate them in each time period, minimizing the maximum number of infected people at the same time and the total infected population. Available data for COVID-19 daily cases was used to adjust the parameters of the SEAIR models in four study cases: Austria, Belgium, Denmark, and Chile. From these, we can analyze how different vaccination schemes are more beneficial for the population as a whole based on different reproduction numbers, interaction levels, and the availability of resources in each study case. Moreover, from these experiments, a strong relationship between the defined objectives is noticed.

1. Introduction

In the history of humankind, various viruses have appeared and will continue to appear. Some of them can cause epidemics such as influenza, HIV, Ebola, and COVID-19. The first appearance of the disease caused by the SARS-CoV-2 virus was recorded in December 2019 in Wuhan, China (Liu et al. [1]). The virus spread rapidly to many other countries, and on 11 March 2020 it was declared a worldwide pandemic (Cucinotta and Vanelli [2]), the fifth documented pandemic since 1918 with H1N1 (Liu et al. [1]). In most pandemic scenarios, the large number of people infected in such a short period of time will collapse most of the world's health systems. This happened during the first months of COVID-19 , as the disease spread in most countries in Europe (Ke et al. [3]).

As the number of infected patients rose, most health workers and infrastructure stood firm, but health workers were forced to decide which patients to treat first, generating not only deaths but also severe psychological effects on the population and even more on the health workers who had to deal directly with this situation. In the current globally connected world and considering the contagiousness of the virus, one infected person can spread the virus to two or three other people. Each country sets different measures to decrease the viral spread and increase social distance. Among the actions taken, borders have been closed, quarantines have been carried out, and activities have been limited to smaller groups of people (Knox et al. [4], Costa-Font and Vilaplana-Prieto [5]) .

Despite rapid advances in vaccine production, at the beginning of the disease a limited number of vaccines were available to use for each country. Officials sought the best way to

use the available vaccines, especially considering the associated production and transportation costs. In this sense, determining the best vaccination plan for SARS-CoV-2 and assessing a limited number of vaccines is a significant problem. This is unlike classical vaccination strategies implemented in most countries during pandemics, which focus on the speed of the vaccination process (Chen [6]) or the vaccination of specific people like health workers and at-risk populations (Goldstein et al. [7], Rimmelzwaan et al. [8], Gu et al. [9]). In this study, we propose a methodology that considers the interactions between subgroups of a population (Gu et al. [9], Keeling and Eames [10], Petrizzelli et al. [11], Varotsos et al. [12]). Moreover, unlike most of these works, we also consider a restricted number of available vaccines and vaccination time periods according to the arrival of batches of vaccines. This approach is formulated based on previous vaccination models for SARS-CoV-2. Moreover, adaptations of previous epidemic models are studied in a way that models SARS-CoV-2 spread in agreement with the available recorded information.

This study presents a methodology by which to determine effective period-based budget-restricted vaccination plans that consider subgroups of populations and their interactions in order to model mobility constraints as a key factor to control the spread of disease. This method applies an epidemic model that takes into account the infected and asymptomatic population, as well as divisions of the population, restriction of population movement, and prohibitions of contact between divisions based on weighted graphs. Before applying these methods, adjustments of the COVID-19 spread parameters and the corresponding motion constraints in each case study are performed in order to obtain models as close as possible to the corresponding recorded COVID-19 data. The vaccination plans determine how many people should be vaccinated per division per period of time considering a restricted number of available vaccines per period, and they use an ad hoc tabu search heuristic approach coupled with the adaptations of the epidemic models studied.

First, in Section 2, we introduce the main epidemiological models in the literature. In Section 3, we introduce and review previous works related to epidemic models and vaccination algorithms. Thirdly, in Section 4, we describe the problem to be solved. Subsequently, we explain our algorithm implementation in Section 5. Furthermore, we describe the instances and experiments made in Section 6. In addition, we analyze the results obtained for four different instances in Section 7. Finally, we analyze the conclusions of our work and define potential future work in Section 8.

2. Epidemiological Models

Epidemic models show how a disease spreads through the population. Thus, they can be used to predict outbreaks and the effect of different methods for controlling, decreasing, or delaying a disease's spread. These epidemic models are generally solved as ordinary differential equations (ODEs), but in some complex cases they can be solved by partial differential equations (PDEs) (Schneckenreither et al. [13]). Epidemic models can be classified according to the steps of their spreading process.

The Susceptible-Infected-Recovered Epidemic model (SIR) (Bacaër [14]) is one of the simplest approaches for modeling disease spread. This model divides the population into three groups, as follows.

- Susceptible (*S*): Healthy individuals who can catch the disease.
- Infected (*I*): Individuals who currently have the disease and can transmit it to susceptible individuals.
- Recovered (*R*): Individuals who had the disease and now are immune.

For the SIR model, it is assumed that (1) the sum of individuals in these three groups corresponds to the population size (*N*). In this way, the model is closed, entailing that the population size is always the same, (2) the contact rate (contact between individuals) per unit of time will be β, (3) after contact with an infected individual, a susceptible individual gets infected with rate C_e and becomes immediately infected (there is no incubation period), and (4) infected individuals recover after r delay of time or recovery rate as $1/r$ (time a

person remain infected). An indicator of the transmission capacity of a virus is settled by the basic reproduction number (R_0), which represents the average number of infections generated by a single person through the population. Different diseases that share the same infectious phases can be modeled by knowing the values of the parameters mentioned above. Birth rate b, death rate d, and disease death rate a can be added to the previous equations too.

The Susceptible-Exposed-Infected-Recovered Epidemic model (SEIR) is a variation of the SIR model (Li and Muldowney [15]). A new group of exposed individuals is incorporated in this case. Referring to some diseases, after contact between a susceptible and an infected person, the susceptible individual becomes exposed. In this state, the person is infected but not infectious (cannot infect susceptible individuals) because of the incubation period of the disease. The factor e represents the rate of exposed individuals becoming infectious. The number of infected individuals depends on the exposed individuals and the rate of becoming infectious.

Another variation of the SIR epidemic model is the Susceptible-Infected-Quarantined-Recovered Epidemic model (SIQR). In this model, some infected individuals are quarantined with a rate q and stop infecting susceptible individuals. Moreover, a constant η is incorporated to represent the recovery rate of quarantined people.

3. Literature Review

Computational systems use three main approaches to model the effects of their strategies in the control of the disease spread: analytical deterministic (Maltz and Fabricius [16]) and stochastic (Fabricius and Maltz [17]) and simulation approaches (Fu et al. [18]).

Analytical models use mathematical models, particularly optimization models, to assist in making decisions. Mathematical programming models can be solved with direct or indirect methods. In direct methods, the discretization scheme is used to transform the optimal control problem into a nonlinear programming (NLP) problem, which an NLP solver can solve. In indirect methods, the solution is derived based on the optimal conditions, leading to a two-point-boundary problem. Epidemic models have been approached in two ways.

- Analytical deterministic approaches allow a closed representation of the spread but require many assumptions. Moreover, these approaches generate a rough model of the current virus spread, but, in most cases, are very sensitive to parameter changes.
- Analytical stochastic approaches are similar to a deterministic model, but in these cases, parameters are modeled statistically. These approaches are less affected by changes in the model parameters.

In simulation approaches, a population graph can be constructed. These approaches incorporate realistic assumptions about a virus's population structure and transmission dynamics. Each node in this network represents a person connected to others following specific relation dynamics. Simulation is computationally time-consuming, so in most cases, straightforward strategies are preferred. This makes it impossible to take into account broad characteristics to divide the population.

Vaccination Models

Some epidemic models have been adapted, adding vaccination to determine epidemic control strategies. Most works implement perfect vaccination, whereby the vaccinated become immune and turn directly into recovered individuals. However, vaccination enforced with normal distribution (Tanner et al. [19]) that uses a stochastic programming approach and with resistance to vaccination (Chen et al. [20]) has been studied.

In Correa Cordova et al. [21], a study with periodic vaccination was conducted. This study allows for multiple pulse vaccinations to be implemented as a control strategy and optimizes the time points at which the population is vaccinated. It also provides for different vaccination levels. They assumed perfect vaccination. The overall problem is solved by an NLP solver based on the solutions and the sensitivities computed in each subinterval.

Vaccination in SIR and SIS models has been implemented by using a relational network graph (scale-free network) in Wu and Lou [22]. Here, they represent the immunized population and apply random vaccination and targeted vaccination strategies. A path parameter was incorporated to be aware of immunizing high-risk nodes. This is the effective method in scale-free networks to vaccinate the nodes with the highest degree, the ones connected to more nodes. This group can be defined as a region or group of people sharing some characteristics. Then, the nodes that must be vaccinated in a graph to decrease or remove the virus are identified.

An evolutionary multiobjective optimization algorithm that uses a stochastic simulation approach was used to determine vaccination policies for a SIR model in da Cruz et al. [23]. In their work, the authors minimize the control costs and the number of infected individuals. In order to express the system as a fraction of each group, the authors divide the equations of a SIR model incorporating birth and death rates in the whole population.

Quarantine has been added as well for vaccination models in Kim et al. [24]. This study aimed to determine and select who should be vaccinated and given a limited number of vaccines. The authors generated a distribution of vaccines over time intervals. In a new vaccine strategy with delivery over time, susceptible individuals who have been vaccinated become immune and turn directly into recovered individuals—also called perfect vaccination and quarantine. This was implemented based on social relationships and prediction of the routes of infection and obtainment of better results for their SVDP solutions than the random distribution of vaccines.

A model for finding optimal vaccination strategies of a constrained time-varying SEIR epidemic model (Wang et al. [25]) was developed. In this model, the population (N) is not necessarily constant as in some previous works. The authors assumed death rate, birth rate, disease death rate, incubation period, and recovery rate as constant values; the vaccination rate is considered the control variable, and the contact rate can vary seasonally as a cosine function. Vaccinated individuals become immune with a specific ratio that decreases in time t, because of drug resistance as a monotonic decreasing function. They define a limited supply of vaccines at each time instant. They prove that omitting time-varying factors may result in an unreasonable vaccination strategy.

Ng et al. [26] developed a multicriteria mathematical programming model to find the optimal combination of influenza vaccination strategies by using a deterministic approach. As performance measures, they considered minimizing the vaccination cost, maximizing the vaccination efficacy by using the postvaccine reproduction number (Halloran et al. [27]), and maximizing societal benefits. Thus, they formulate a multicriterion optimization problem and search for nondominated solutions, focusing on determining the optimal number of vaccine doses to be assigned to different population groups at risk.

Optimizing vaccination with exposed individuals and incorporating a quarantine factor has also been done by Enayati and Özaltin [28]. In this work, the population is separated into subgroups. Each subgroup has its proportion of susceptible (S), exposed (E), infected (I), quarantined (Q), and recovered (R) individuals. The authors change the generic contact rate of the SEIR model to define a more specific contact rate between subgroups. These values also determine the rate of new infections in each subgroup. They use a nonlinear mathematical model, minimizing the total number of doses.

4. Problem Description

This section describes the problem to be solved as a susceptible (S), exposed (E), infected (I), asymptomatic (A), and recovered (R) model with subgroups, vaccination, and restrictive measures that change according to the quantity of infected population.

The model obeys the following obligatory rules.

- Birth rate is equal to the death rate.
- Exposed individuals are split into infected and asymptomatic individuals with their perspectives rates.
- A fraction of asymptomatic individuals are tested and move to infected individuals.

- There is a limited quantity of vaccines.
- Population is divided into subgroups. This division can be based on geographical zones or political divisions like cities or districts.
- Each zone has a contact rate with itself and all other zones. These contact rates can be interpreted as the percentage of people in the group staying in the area and the percentage of people visiting, traveling, or working in another zone.
- Each country has restricted the movement of the population. Chile has used a strategy in which each district has more restrictions based on the number of infected people. For this, the population in each subgroup decreases their contact rate according to their infection level. In this work, for each zone will, Equations (17) and (18) will resemble this behavior.
- Infected population decreases its movement considering an equal or higher rate than the infected people.

Additionally, vaccination over periods is implemented. The approach implements just one vaccination period at the beginning of the epidemic. It searches only for the best vaccination plan with a fixed quantity of vaccines to assign to different subgroups every period.

The model phases of the population are shown in Figure 1. Susceptible individuals become exposed individuals because of their interaction with infectious populations. The infectious population can be considered infected individuals with infection rate β and asymptomatic individuals with infection rate α. Exposed individuals become infectious with a rate of δ. A μ fraction of the infectious population is asymptomatic, and $1 - \mu$ shows symptoms. From the asymptomatic population, some of them are tested with rate η and start showing as infected. Infectious people recover with rate γ.
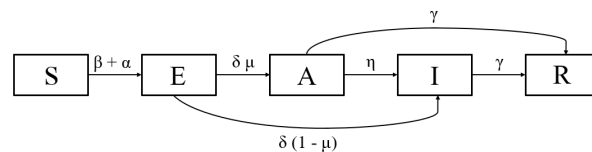

Figure 1. SEAIR model. S, E, A, I, R corresponds to susceptible, exposed, asymptomatic, infected, and recovered populations.

To model the interactions between subgroups in the population, we assume that:

- People from each subgroup can visit any other subgroup. These visits can primarily be workplace visits.
- The percentage of people that move to another subgroup is represented on a contact matrix, which sums 100% per each subgroup.
- For any subgroup x, subgroup x' corresponds to the group formed by all the population that visits subgroup x, excluding the population from subgroup x that visits other subgroups.
- The newly infected population of subgroup x' is obtained from the contact between infected and susceptible people of subgroup x'.
- The newly infected population of subgroup x is computed as the sum of all newly infected individuals from subgroup x who visit other subgroups and the newly infected people who stay in subgroup x.

Mathematical Model

The previously explained rules are fulfilled through the following mathematical model. Next, we list the parameters of the model.

N	Population size
G	Set of subgroups
V	Quantity of vaccines available per period.
T	Total time considered.
ζ_{ij}	Percentage of people from subgroup i who visit subgroup j (contact matrix).
β_{ij}	Infectious rate between subgroup i and j.
α_{ij}	Infectious asymptomatic rate between subgroup i and j.
δ	Incubation rate. Days of incubation on an exposed individual to become infectious.
γ	Recovery rate. Days of an infectious individual (infected or asymptomatic) to become recovered.
η	Detection of asymptomatic rate. The detection based on how many tests are performed on asymptomatic individuals also depends on the real number of asymptomatic individuals.
μ	Percentage of infectious individuals that are asymptomatic.
MIP_α	Percentage of the maximum infected people of the subgroup that triggers movement restrictions of the noninfected population of the subgroup (i.e., quarantine).
MIP_β	Percentage of the maximum infected people of the subgroup that triggers movement restrictions of the infected population of the subgroup (i.e., quarantine). More restrictive measures should be implemented for infected people.

The model defines the variable v_{ip} as the number of persons from subgroup i who will be vaccinated in period p.

Next, we list the constraints of the model. Here, we first list the classical SEIR model constraints (from Equations (1) to (6)), then the contact rate constraints (from Equations (7) to (14)), and the vaccination constraints (from Equations (15) and (16)). We have

$$N = S(t) + E(t) + A(t) + I(t) + R(t) \tag{1}$$

$$\frac{dS_i}{dt} = -\sum_{j=0}^{G} \left(\frac{\zeta_{ij}(t)\,S_i(t)}{\sum_{k=0}^{G}\left(N_k\,\zeta_{kj}(t)\right)} \left(\sum_{k=0}^{G} \left(\beta_{kj}(t)\,I_k(t) + \alpha_{kj}(t)\,A_k(t) \right) \right) \right) \tag{2}$$

$$\frac{dE_i}{dt} = \frac{dS_i}{dt} - \delta\,E_i \tag{3}$$

$$\frac{dA_i}{dt} = \mu\,\delta\,E_i - \gamma\,A_i - \eta\,A_i \tag{4}$$

$$\frac{dI_i}{dt} = (1 - \mu)\,\delta\,E_i + \eta\,A_i - \gamma\,I_i \tag{5}$$

$$\frac{dR_i}{dt} = \gamma\,(I_i + A_i). \tag{6}$$

Equation (1) establishes that the population should maintain its size. Equation (2) controls the susceptible population of each subgroup that becomes infected depending on their contact rate with infected individuals in other subgroups and themselves. Equation (3) controls the exposed individuals per each subgroup that becomes infected or is asymptomatic after incubation. Equation (4) computes the fraction of exposed individuals of each subgroup that become asymptomatic individuals. Equation (5) computes the fraction of exposed individuals of each subgroup who tested as positive COVID-19 cases and become

infected individuals. Equation (6) controls the number of infected and asymptomatic individuals per subgroup that recover after the recovery period. We have

$$\zeta_{ij}(t) = \zeta_{ij}(0) \, F_{\alpha i}(I_i(t)) \tag{7}$$

$$\beta_{ij}(0) = R_0 \, \gamma \, \zeta_{ij}(0) \tag{8}$$

$$\beta_{ij}(t) = \beta_{ij}(0) \, F_{\beta i}(I_i(t)) \tag{9}$$

$$\alpha_{ij}(t) = \beta_{ij}(0) \, F_{\alpha i}(I_i(t)) \tag{10}$$

$$\alpha_{ij}(t) \geq \beta_{ij}(t) \tag{11}$$

$$F_{\alpha i}(I_i(t)) \approx 1 \, ; \, I_i(t) << N \tag{12}$$

$$F_{\alpha i}(I_i(t)) = \frac{100}{100 + A_1^{-B_1 \frac{I_i(t)}{MIP_\alpha N_i}}} \tag{13}$$

$$F_{\beta i}(I_i(t)) = \frac{100}{100 + A_2^{-B_2 \frac{I_i(t)}{MIP_\beta N_i}}}. \tag{14}$$

Equation (7) establishes that people who move from subgroup *i* to subgroup *j* decrease because of government regulations that depend on the quantity of infected. Equation (8) controls infection rate between subgroups (Beta) is obtained from the R_0 value, the recovery rate, and the contact between them. Equations (9) and (10) control the decrease of contact rate of infected and asymptomatic people due to government regulations, respectively. Equation (11) controls that the contact rate of infected is lower or equal to the asymptomatic people. Equation (12) keeps contact regular when there are no (or few) infected people. Equations (13) and (14) establish that government restrictions can be triggered when there is a high number of infected individuals. People increase their movement for mental health reasons and work responsibilities when the infected population decreases. We have

$$S_i(t_p) = S_i(t_{p-1}) + \frac{dS_i}{dt} - v_{ip} \tag{15}$$

$$R_i(t_p) = R_i(t_{p-1}) + \frac{dR_i}{dt} + v_{ip}. \tag{16}$$

At the beginning of each vaccination period, the vaccinated people recover immediately. This is controlled by Equations (15) and (16).

With regard to our objective function, in this work, two objective functions can be considered: the minimization of the number of infectious people in all the periods listed in Equation (17) and the minimization of the number of infectious people at the same time listed in Equation (18). We have

$$Obj_P = min \, \{I(t_f) - A(t_f)\} \tag{17}$$

$$Obj_S = min \, \{max_t\{I(t) + A(t)\}\}. \tag{18}$$

5. Solution Method

This section describes the tabu search algorithm used to get an efficient vaccination plan for a fixed number of available vaccines and periods. The tabu search is a well-known local search metaheuristic method (Glover and Laguna [29]). It has been used to successfully solve several similar optimization problems in the literature (Glover and Laguna [29], Liang and Chao [30], Euchi [31]). Moreover, it is an algorithm that is not highly time consuming compared to population-based methods like evolutionary and swarm-based approaches. This is specially important given the time-consuming evaluation procedure the algorithm implements.

Solutions are represented as arrays of vaccination distributions. The size of each solution depends on both the number of subgroups (G) and the number of periods (P). Each cell indicates the number of vaccines allocated to each subgroup in each period. Figure 2 shows an example of solution for a problem that considers five subgroups, two periods, and 100 vaccines per period.
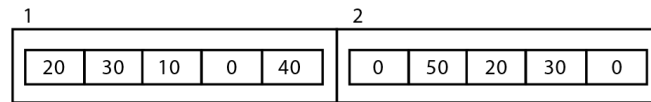
1						2				
20	30	10	0	40		0	50	20	30	0

Figure 2. Example of a solution representation for a problem with five subgroups, two periods, and 100 vaccines per period.

Two objective functions are considered, the minimization of the quantity of infected population at the same time (Obj_P) and the minimization of the number of infected people in the whole period (Obj_S). From this, we define the evaluation function as a weighted sum of both objectives, as shown in Equation (19). Parameter α sets the relative weight of each function during the evaluation process.

$$\alpha * Obj_P + (1 - \alpha) * Obj_S \tag{19}$$

5.1. Algorithm Structure

The approach proposed is a local search-based approach that separates each problem according to the number of periods it considers. As shown in Algorithm 1, for each period, an initialization, a local search, and a completion step are performed. The process starts defining the initial values of the period, the quantity of susceptible, exposed, infected, asymptomatic, and recovered population at the beginning of the current period (line 1). Next, an initial solution is constructed with an initialization (line 5). A local search process is then performed on the constructed solution. This method returns the best solution found during its search (line 6). The best previous solution found is set as the vaccination for that period (line 7) and used to get the initial values of the next period (line 8). The previous process is performed for each period in the problem instance. The final result contains the complete vaccination plan for all periods.

Algorithm 1: SEAIRV Search

Input　:Population, R_0, Gamma, Delta, Eta, ContactMatrix
Output:Vaccination distribution for each period

1　nextInit ← setInitialvalues(input)
2　completeSolution ← Empty list
3　**foreach** *Period* **do**
4　　init ← nextInit
5　　sol ← initializeSolution(Method, init)
6　　sol ← localSearch(sol, iterations, Stopcriteria)
7　　completeSolution ← Add(sol)
8　　nextInit ← setInitialvalues(sol)
9　**end**

Initialization

Five methods were evaluated to construct initial solutions. The initialization methods proposed are listed below.

- All to One: This method allocates all the vaccines of the period to just one subgroup. For this, it evaluates all the subgroups and selects the option that obtains the best evaluation function.

- Inner Interaction: This method allocates vaccines to each subgroup proportionally to the interaction between other subgroups and the current one. It starts computing the sum of all the interactions from different subgroups to the current subgroup. Then, it calculates the percentage according to the value of inner interaction per subgroup.
- Outer Interaction: This method allocates vaccines to each subgroup proportionally to its interaction with the other subgroups. It starts computing the sum of all the interactions from the current subgroup to different subgroups. Then, it calculates the percentage according to the value of outer interaction per subgroup.
- Mixed Interaction: This method allocates vaccines to each subgroup proportionally to the other groups' interaction with the current one and its interaction with the different subgroups. It starts computing the sum of all the interactions from the actual subgroup to different subgroups and other subgroups to the actual subgroup. Then, it calculates the percentage according to the value of outer interaction per subgroup.
- Equity: This method allocates vaccines equitable to all subgroups in the problem instance. For this, we give each subgroup the same probability of getting a vaccine. Then, it allocates vaccines following a uniform distribution.

5.2. Local Search

The local search process is shown in Algorithm 2. It is based on the tabu search metaheuristic. At the beginning of the process, an empty tabu list is considered (line 3). The search considers as stopping criteria a maximum number of iterations and a stuck criterion (line 4). This last criterion is evaluated as the number of iterations without changing the current best solution. At each iteration, a new solution is generated (line 6) by using one of the possible movements generated with a random function with probabilities for each (line 5). The applied movement is recorded into the tabu list (line 6). The tabu list records a pair formed by the subgroups that trade vaccines. For example, if a movement was generated between subgroup 2 and subgroup 6, without regarding the movement type, it records the tuple (6,2) because subgroup 6 can not return vaccines to group 2. Neither a swap nor an inversion can be performed between them.

Moreover, if the obtained solution is better than the actual best, the best solution is updated. In another case, the number of iterations without improvement is increased (line 7). At the end of the process, it returns the best solution found.

Algorithm 2: Local Search

    Input : sol, Iterations, Stopcriteria
    Output: Vaccination distribution for one period

1 iter ← 0
2 withoutChange ← 0
3 tabuList ← Empty list
4 **while** *Iterations > iter AND Stopcriteria > withoutChange* **do**
5   movType ← randomMovType()
6   sol, tabuList ← generateMovement(movType, tabuList, Objective)
7   withoutChange ← withoutChange + 1
8   **if** *bestValue > Evaluation function (sol)* **then**
9   bestValue ← value(sol)
10   bestVaccination ← sol
11   nextInit ← initialValues(sol)
12   withoutChange ← 0
13   **end**
14 **end**

Three different movements were implemented.

5.2.1. Give Random

The idea here is to reallocate the number of vaccines between subgroups. One random subgroup (sg) with at least one vaccine allocated is selected. In addition, a random quantity between 1 and the number of vaccines (v) currently allocated to (sg) is chosen. These v vaccines are reallocated from sg to each other subgroup. Each possible change is considered a neighbor solution. The first new allocation that shows a better evaluation function is selected by considering a first improvement approach. Moreover, if it is not possible to get any improvement, a best improvement approach is considered by selecting the best option.

5.2.2. Swap Random

The idea of this movement is to diversify the search and have chances of a faster convergence by finding new solutions in the case of being stuck into local optima. For this, two random subgroups with different quantities of vaccines are selected to swap all their vaccines with the other subgroup. In this case, the neighborhood is constructed by applying this movement five times, every time for two random subgroups.

5.2.3. Invert Random

The idea of this movement is to diversify the search and allow a faster convergence by finding new solutions in the case of being stuck into local optima. For this, two random subgroups are selected, and an inversion of the number of vaccines to all the subgroups between them is performed. This works similarly to a mirror effect, and the neighborhood is constructed again by applying the movement five times between different random selected subgroups.

6. Computational Experience

6.1. Data Selection

To select instances to evaluate, data from countries with high coronavirus testing and a variegated population and division was selected.

The number of tests and daily cases of countries were obtained from ourworldindata.org [32], open access and open source databases for research and media, and for the Chilean metropolitan region from coronavirus.mat.uc.cl [33]. COVID-19 data wa obtained from the Chilean Ministry of Science and Technology and processed for Data UC. The chosen data, and consequently the created instances for this work, were constructed based on data from four countries: Austria, Belgium, Denmark, and Chile. Preliminary experiments were also executed by using the metropolitan region of Santiago, Chile.

- Austria: Nine states, a population of 8,935,112 and 1577.72 COVID-19 tests per 1000 people.
- Belgium: Eleven provinces, a population of 11,431,406 and 809.87 COVID-19 tests per 1000 people.
- Denmark: Five regions, population of 5,840,045 and 2841.41 COVID-19 tests per 1000 people.
- Chile: 16 regions, population of 17,574,003 and 481.44 COVID-19 tests per 1000 people.

6.1.1. Setup

Each problem instance requires the definition of the scenario analyzed. In each case, we required consideration of the number of subgroups, the population, recovery rate (γ), reproduction number (R_0), incubation rate (δ), percentage of asymptomatic infected people (μ), detection of asymptomatic people (η), and the contact matrix. Next, it is explained how these components were determined for each instance.

The number of subgroups is created based on the divisions per country. For each input file, the total population and subgroup populations were set based on the population size and division sizes obtained from different sources of their past census. This was in order to set a population value closer to reality.

Contact matrices were created by using a two-step procedure. First, an initial contact matrix was created based on a weighted random graph.

There are different methods like Erdös–Rényi or Barabási–Albert to create random graphs. For more information about different methods to create random graphs Gao [34], Volchenkov and Blanchard [35], Vega Yon et al. [36] can be revised. The method used in this work is similar to the Bianconi–Barabási model. It consists of assigning each subgroup to one of the three types of nodes according to its betweenness centrality (how strong a connection it has with other subgroups). The first type of node has the highest betweenness centrality, the second type has medium betweenness centrality, and the third type has the lowest betweenness centrality. The number of nodes of each type is computed based on how many main divisions the population has. For example, in Chile there is only one main division, the metropolitan region with almost 41.89% of the population from 16 divisions. Then, there are other six divisions corresponding to medium betweenness nodes and the remaining divisions have low betweenness nodes. From the previous distributions, contact values are generated with random values based on their node betweenness. Nodes with high betweenness will get higher values than those with low betweenness, keeping the sum of all these contacts per subgroup to 1. For all the countries, the inner interaction of the node is set to a value between 0.4 and 0.6, given that a large fraction of the population in these big divisions work or visit the same division.

After the contact matrix is created, the values per each subgroup can recreate the distribution of contacts with other subgroups but not necessarily with the correct subgroups. In order to get closer to the real situation, a geographical adjustment step is performed based on their proximity.

There is a rule for nonadjacent divisions with the intention of maintaining the betweeness of all subgroups. In the case of nonadjacent divisions, if one of them has a higher degree or is a node of high betweeness centrality, then the subgroup will get the highest value. After these two steps, the final contact matrix is obtained for its use in the SEAIRV model.

6.1.2. SEAIR Curve Adjustments per Input Data

The parameters to adjust are divided in two: the COVID-19-based parameters, i.e., parameters that depend on the virus, and the SEAIR parameters created to resemble as much as possible the local reality related to the restrictions and movements of the population.

COVID-19 Parameters

Once the parameters related to the number of subgroups, the population size, and the contact rate matrix of Section 6.1.1 are defined, it is necessary to adjust the parameters of the SEAIR models to the real data curves of COVID-19.

Some of the parameters needed are obtained directly from the disease characteristics. These are the incubation rate (δ), recovery rate (γ), and percentage of infected that are asymptomatic (μ), although they may vary depending on each person. There are two other parameters that are related to the disease—the basic reproduction number R_0, which depends on the way of contact of the disease (air, blood), and the contact of the population, and the detection of asymptomatic (η) that will depend on how COVID-19 testing is performed. For these five parameters, the range values of four of them—δ, γ, μ, R_0—were determined from two sources, the Centers for Disease Control and Prevention (CDC) [37] and The Centre for Evidence-Based Medicine (CEBM) [38]. The parameter η depends on each country having a range between 5% and 80% that is seated.

The ranges of the parameters are shown in Table 1. The first column correspond to the name of the parameter. The second, fourth, and sixth columns correspond to the minimum, average, and maximum quantity in days or percentage, each of them followed by the corresponding parameter value.

Table 1. Parameter values ranges based on estimated values from CDC and CEBM.

Parameter	Minimum	Value	Average	Value	Maximum	Value
δ	2 days	0.5	5–6 days	0.2	14 days	0.07
γ	12 days	0.08	2 weeks	0.07	6 weeks	0.024
μ	10%	0.1	40%	0.5	70%	0.7
η	5%	0.05	30%	0.3	80%	0.8
Initial R_0	2	2	3	3	6	6

SEAIR Parameters

From the SEAIR Model there are six parameters to set for each input file. The parameters are A_1, B_1, and MIP_α for the movement function of the noninfected individuals in populations (including asymptomatic) and A_2, B_2, and MIP_β for the movement function of infected individuals in the population. The parameters A_1, B_1, A_2, and B_2 are related to the inclination and variation of the data curve due to small changes in the number of those infected. For this, eight possible combinations of the four values that maintain the quantity of infected people (and which are close to the maximum quantity of the infected population for the subgroup) were seated. The parameters MIP_α and MIP_β define the maximum percentage of the population, noninfected and infected, respectively, allowed to apply a quarantine. Due to this, their values can change between countries according to how restrictive the measures are in terms of population movement.

Adjustments

To set all the previous parameters, we seek to have them resemble as much as possible the SEAIR curve with the real COVID-19 data. Figure 3 shows a curve of newly infected individuals per day. Two curves are shown here. The blue curve shows the data coming from information systems, and the violet curve shows the SEAIR model. The x-axis shows the days, and the y-axis the total population. It can be seen how the SEAIR curve and the COVID-19 curve have similarities after the adjustment process. Both of these epidemic curves have a peak—the highest value—at approximately 17,500 newly infected individuals. Both curves show a specific time during which a high increase in the number of cases can be identified (close to day 75). Furthermore, the way the curve decreases after the peak can be really prominent, reaching values close to zero. In some cases, this decrease can be slower and converge to an equilibrium state of the number of infected people. Curves of different scenarios are different; hence, it is not always possible to get a close-fitting curve to the original one. Despite this, the adjustment process searches for a set of parameters that lead to the most similar curve.

It starts seating the COVID-19 parameters in the average values and the SEAIR parameters in the first possible combination of A_1, B_1, A_2, and B_2, and for MIP_α and MIP_β a value of 0.02 and 0.005.

After this, the COVID-19 values are increased or decreased, prioritizing the change of the R_0 and η values because these are based on features of the population. Moreover, the other three values can be changed without trying to set them far away from the average value. These changes are performed until the peak of both curves (real data and SEAIR model curve) are positioned similarly in the same day (with respect to to the x-axis) and also how flat/extended is the curve. Basically, δ, γ, and R_0—with highest values—move the peak of the curve to the left (because it is more exponential in that case) and also make the amplitude higher. The longitude and amplitude of the curve is related to all the parameters in a greater or lesser way.

With the COVID-19 parameters set, it is possible to change the MIP_α and MIP_β values. MIP_β determines the maximum quantity of infected or the peak (highest value) of the curve, and MIP_α determines how the curve decreases after the peak and also if it reaches equilibrium or tends to zero. The combination of A_1, B_1, A_2, and B_2 parameters gives more

or less amplitude to the curve. It also gives a bigger or smaller fall of the curve after the peak, and in the case of equilibrium, a greater or lesser difference with regard to the value of the peak.
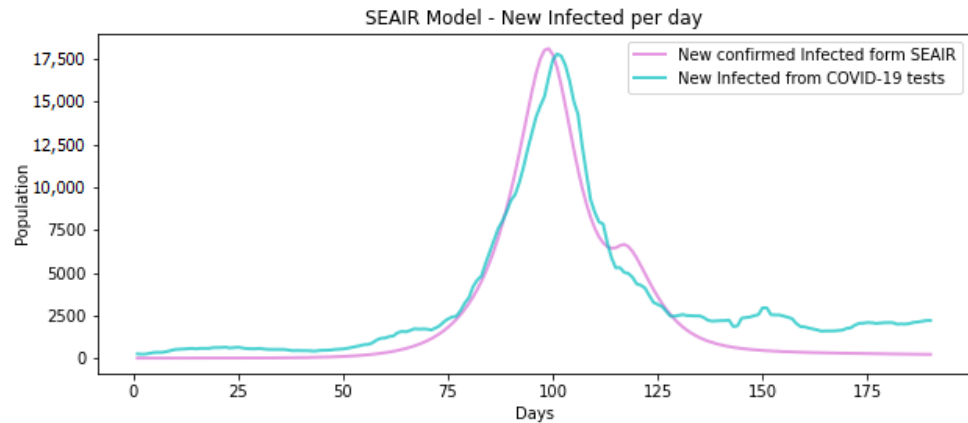

Figure 3. Example of newly infected persons per day data and SEAIR adjusted curve in Belgium. Second wave.

The data files of Austria, Belgium, and Denmark were adjusted to the second wave and the Chilean data was adjusted to the first and second wave. This, due to the peak of the curve, is higher in the first wave in this case. The restrictive values for the infected population (MIP_β) are between 0.0100 and 0.0030 and those for the noninfected population (MIP_α) are between 0.1 and 0.02 of the division population. For the combination of parameters A_1, A_2, B_1, and B_2, the infected curve of the values $A_1 = 0.010$ and $B_1 = 1.1$ are the most used. For the noninfected curve, the values $A_2 = 0.001$ and $B_2 = 1.0$ are seated for most cases. Furthermore, the best vaccination plan in the case of covers between 9.48% in the worst case and 31.19% in the best case. The R_0 obtained for the cases that are fitted to their first wave are much higher than the other values due to the fact that the number of tests that were conducted at the beginning of the pandemic was lower, resulting in the need to use a higher R_0, which increases the quantity of the infected population moving the corresponding curves much more quickly to the left.

6.2. Experiments

In order to set the parameters of the algorithm of the SEAIRV model, three experiments were analyzed. The objective of the first experiment was to evaluate the relevance of the three proposed movements into the local search approach proposed. The second experiment is focused on evaluating the three initialization methods proposed. The last experiment evaluates the two objective functions studied in this approach.

Each experiment was executed 30 times considering the stochastic nature of the tabu search approach. Each one considered a maximum of 100 iterations and a stopping criteria of 30 iterations without improvement of the best solution. Tabu search list size was fixed to 20% of the corresponding vaccination plan size. These parameter values were mainly fixed based on preliminary experiments. Due to the extensive computational times required by the method, we fixed a low number of maximum iterations ensuring that convergence is reached in most cases.

6.2.1. Movement Relevance

For this experiment, we evaluate a set of six probabilities values for the tree movements: Choose a subgroup and give a random quantity of vaccines (Give Random), change the quantity of vaccines between two subgroups (Swap Random) and invert all the vaccines between two subgroups as a mirror (Invert Random) that were explained in Section 5.2.

Each experiment was executed 30 times. Each one considered a maximum of 100 iterations, a stopping criteria of 30 iterations without improvement of the best solution and initialization of the Inner Interaction. This process was made for six different parameter configurations.

6.2.2. Initialization Procedures

The second experiment was for setting which of the initialization processes—All to One, Inner Interaction, Outer Interaction, Mixed Interaction, or Equity, as explained in Section 5.1—to use. Again we made 30 runs of the algorithm with 100 iterations and a end criteria of 30 iterations without changing the best solution. In this case, the previously set distribution of the movements were 80%, 10%, 10%.

6.2.3. Objective Functions

The last test is focused on analyzing the factors to optimize—Maximum Infected at the same time and Total Infected in the period of the objective function, as explained in Equation (19) of Section 5. This execution is to run 30 times for the algorithm with 100 iterations and an end criteria of 30 iterations without changing the best solution by using the previously seated movement distribution and initialization.

6.2.4. Vaccination Plan per Input Data

Experiments were made per each input file. As before, each experiment was executed 30 times, choosing the best solution obtained from the 30 executions. Each one considered a maximum of 100 iterations and a stopping criteria of 30 iterations. Moreover, each iteration had the parameters of movements for Give Random at 80%, Swap Random at 10%, and Invert Random at 10%. This wa accomplilshed by using the All to One initialization and objective functions seated at 50% and 50%.

7. Results

This section presents the results of the experiments. It is composed of the SEAIRV parameter results and the vaccination plans for different problems.

All experiments were executed on a computer with an AMD Ryzen 5 3600 6-Core Processor running at 3.60 GHz, using 16 GB RAM in Windows version 22H2. The code was executed in Jupyter notebook 6.5.2. using the library scipy version 1.10.0.

7.1. SEAIRV Parameter Setting Results

The results of the three experiments to determine SEAIRV parameters are shown and explained below. Each of them has its own table showing results, description, and interpretation.

7.1.1. Movements Relevance

Six parameter configurations were tested to evaluate the relevance of the movements in the algorithm's performance. Each one represents the probability of use of the three proposed movements: Give Random, Swap Random, and Invert Random. From preliminary experiments, we selected for study the following parameter configurations: $c_1 = 30 - 40 - 30$, $c_2 = 40 - 40 - 20$, $c_3 = 80 - 10 - 10$, $c_4 = 80 - 20 - 0$, $c_5 = 90 - 5 - 5$, and $c_6 = 100 - 0 - 0$ for Give Random, Swap Random, and Invert Random, respectively. Table 2 shows the average execution time and the average number of infected obtained by each parameter configuration in each case and their corresponding standard deviation.

The first column of the table corresponds to the input data name, and the second column shows the configuration identification; then the corresponding average execution time in seconds and the average maximum infected resulting from 30 executions and their corresponding standard deviation are shown. Each one considers a maximum of 100 iterations and stopping criteria of 30 iterations without improvement of the best solution.

For three of the four files—Belgium, Austria, and Denmark—the use of only one movement, Give Random (configuration c_6) shows the best quality, but for Chile, it is the opposite. In Chile, the worst number of infected was obtained with this configuration. In terms of time, there is not a significant difference or any observable pattern related to the probability of the movement for the Belgium and Denmark files, but for Chile and Austria the execution time increases with the use of the movement Give Random. Still, it can be noticed that depending on the number of subgroups, the time taken to obtain the solutions increases.

Table 2. Average time and maximum infected population obtained per country file for different probabilities of the movements. The best value per file is highlighted in bold.

Input Data	Configuration	Average Time [s]	Average Maximum Infected
Austria	c_1	**139**	30,392.8 ± 416
	c_2	146	30,169.8 ± 370
	c_3	170	29,426.7 ± 401
	c_4	178	29,430.8 ± 450
	c_5	184	29,138.2 ± 345
	c_6	200	**28,968.2 ± 321**
Belgium	c_1	**233**	166,553.210 ± 119
	c_2	240	166,464.9 ± 165
	c_3	286	166,157.8 ± 238
	c_4	292	166,156.1 ± 303
	c_5	308	166,045.5 ± 296
	c_6	319	**165,623.0 ± 309**
Denmark	c_1	54	3202.901 ± 25
	c_2	49	3189.4 ± 25
	c_3	**48**	3156.8 ± 13
	c_4	49	3157.3 ± 10
	c_5	49	3155.7 ± 13
	c_6	52	**3149.9 ± 6**
Chile	c_1	**391**	**125,554.613 ± 78**
	c_2	439	125,601.3 ± 122
	c_3	595	125,799.9 ± 351
	c_4	617	125,966.4 ± 230
	c_5	643	126,038.0 ± 272
	c_6	620	126,205.0 ± 241

Although using only one movement in three of the four cases shows the best performance, using only one movement in the search process can result in poor performance in other problem instances (like Chile, in this case). It can be suggested that the use of only one movement does not allow enough diversification during the search process. This can enable a fast convergence to local optima and premature search stagnation.

Wilcoxon signed-rank tests were also executed on results from Table 2. Table 3 summarizes these results. Here, asterisks show pair comparisons where statistical differences with 95% confidence were found.

A difference between the configuration c_1 and c_2 with 95% confidence was not found for any file; this may be due to the fact that neither of these configurations prioritize any specific movement. Configuration c_6 obtained significantly different results compared to all other configurations. Configurations c_1 and c_2 are considerably different with the other configurations for all instances.

To maintain the use of all movements while prioritizing the move Give Random, which gave the best results in three out of four instances; for the following experiments, we consider parameter configuration c_3.

Table 3. Wilcoxon comparison for different probabilities of the movements results. Asterisks indicate each comparison where a statistical difference with 95% confidence was found.

	Austria						Belgium						Denmark						Chile					
	c_1	c_2	c_3	c_4	c_5	c_6	c_1	c_2	c_3	c_4	c_5	c_6	c_1	c_2	c_3	c_4	c_5	c_6	c_1	c_2	c_3	c_4	c_5	c_6
c_1	-	-	*	*	*	*	-	-	*	*	*	*	-	-	*	*	*	*	-	-	*	*	*	*
c_2		-	*	*	*	*		-	*	*	*	*		-	*	*	*	*		-	*	*	*	*
c_3			-	-	*	*			-	-	-	*			-	*	*	*			-	-	-	*
c_4				-	*	*				-	-	*				-	-	*				-	-	*
c_5					-	*					-	*					-	*					-	*
c_6						-						-						-						-

7.1.2. Initialization Procedures

Here, we evaluate the initialization process's relevance to the proposal's performance. Five initialization methods were proposed: All to One, Inner Interaction, Outer Interaction, Mixed Interaction, and Equity. Each experiment was executed 30 times, considering a maximum of 100 iterations and stopping criteria of 30 without improvement. Moreover, in this experiment, the movement probabilities were seated as c_3. Table 4 shows the results of these experiments.

Table 4. Average time and maximum infected population obtained per country file for different initialization procedures. The best value per file is highlighted in bold.

Input Data	Initialization	Average Time [s]	Average Maximum Infected
	All to One	**134**	**28,657.059 $\pm$ 0**
	Inner Interaction	170	29,426.7 $\pm$ 401
Austria	Outer Interaction	165	29,359.6 $\pm$ 400
	Mixed Interaction	155	29,138.2 $\pm$ 313
	Equity	180	29,428.9 $\pm$ 544
	All to One	**237**	**165,184.1 $\pm$ 0**
	Inner Interaction	286	166,157.8 $\pm$ 238
Belgium	Outer Interaction	295	166,177.1 $\pm$ 283
	Mixed Interaction	290	165,869.9 $\pm$ 295
	Equity	312	166,162.5 $\pm$ 313
	All to One	**33**	**3146.7 $\pm$ 0**
	Inner Interaction	48	3156.8 $\pm$ 13
Denmark	Outer Interaction	48	3158.2 $\pm$ 16
	Mixed Interaction	45	3152.0 $\pm$ 7
	Equity	48	3156.0 $\pm$ 10
	All to One	**423**	126,665.0 $\pm$ 0
	Inner Interaction	595	125,799.9 $\pm$ 351
Chile	Outer Interaction	642	**125,773.9 $\pm$ 302**
	Mixed Interaction	606	126,135.6 $\pm$ 222
	Equity	612	125,897.7 $\pm$ 193

The first column of the table corresponds to the problem instance; the second column is the initialization method used, and the corresponding average time in seconds and average maximum infected as a result of the 30 executions are listed next.

In this case, the best value for three of the four instances: Belgium, Austria, and Denmark, was obtained by using the All to One initialization procedure. Moreover, in all cases, the execution time using the All to One strategy is lower than the execution times obtained by using any other initialization method. This may be due to faster convergence or stagnation of the search process. Despite the time, again for the Chile instance, the worst quality was obtained by using the All to One procedure.

In this case, we also computed the Wilcoxon signed-rank tests on results from Table 4. Table 5 summarizes these results. Here, asterisks show pair comparisons where statistical

differences with 95% confidence were found. AO indicates All to One, II indicates Inner Interaction, OI indicates Outer Interaction, MI indicates Mixed Interaction, and Eq indicates Equity initialization.

For the initialization, Inner Interaction had a 95% confidence, and a difference between every other initialization was found for each instance. The same can be observed for initialization Mixed Interaction but only for three of the four instances. Despite the best average result, for the instances of Austria, Belgium, and Denmark it was found that for All to One the initialization difference was demonstrated only against Inner Interaction and Mixed Interaction.

For the results of the Chile case with regard to the All to One initialization and the results from previous analyses, the initialization was set to All to One for the following experiments.

Table 5. Wilcoxon comparison for different initialization procedures results. Asterisks indicate each comparison in which a statistical difference with 95% confidence was found.

	Austria					Belgium					Denmark					Chile				
	AO	II	OI	MI	Eq	AO	II	OI	MI	Eq	AO	II	OI	MI	Eq	AO	II	OI	MI	Eq
AO	-	*	-	*	-	-	*	-	*	-	-	*	-	*	-	-	*	-	-	-
II		-	*	*	*		-	*	*	*		-	*	*	*		-	*	*	*
OI			-	*	-			-	*	-			-	*	-			-	-	-
MI				-	*				-	*				-	*				-	*
Eq					-					-					-					-

7.1.3. Objective Functions

This experiment aims to analyze the performance of the approach concerning the two objective functions defined: minimizing the quantity of infected population at the same time and minimizing the number of infected people in the whole period. The experiments were executed by using the same parameter values of the previous experiments: movement probabilities c_3 and All to One initialization. Table 6 shows the results obtained for these experiments. Values of α parameter were selected from $\{0, 0.2, 0.5, 0.8, 1\}$, setting the influence of each objective function.

The first column of the table corresponds to the problem instance; the second and third columns show the percentage in the evaluation function to minimize the maximum number of infected at the same time and to minimize the total infected in the period. After this, the corresponding average time in seconds, average evaluation function value (obtained from Equation (19)), average maximum infected, and average total infected as a result of the 30 executions. Standard deviations were not included in this table because in all cases its value was very close to 0.

In this case, the majority of the executions obtained the same values for maximum number of infected individuals and the total number of infected individuals for different weighing values. In the study case of Austria and Denmark, when the objective function gives 100% priority to the maximum number of infected, a very slight improvement in the maximum number of infected was achieved. In the case of Denmark, we prioritize the maximum number of infected and also lightly improve the total infected value. For the Chile instance, a 100% priority of the maximum number of infected or the total infected shows a small improvement in the total infected. It can be seen that the improvement of the value in one of the objective functions does not necessarily improve the value of the other objective function. Additional experiments, not included in this paper, show a small but noticeable tradeoff between the objective functions. These were obtained by using different initialization procedures that lead the algorithm search to different areas of the search space. For the remaining experiments, we used a 50%, 50% balance to consider both objectives having the same relevance.

Table 6. Average time, maximum infected as MI, total infected as TI, and average function value per problem for different weighing in the evaluation function. The best time per file is highlighted in bold, and the best objective function value is shown in bold.

Input data	Percentage of MI	Percentage of TI	Average Time [s]	Average Function Value	Average MI	Average TI
	100%	0%	**133**	28,657.0	**28,657.0**	48,154.5
	80%	20%	142	32,556.5	28,657.1	48,154.5
Austria	50%	50%	137	38,405.8	28,657.1	48,154.5
	20%	80%	136	44,255.0	28,657.1	48,154.5
	0%	100%	149	48,154.5	28,657.1	48,154.5
	100%	0%	237	165,184.1	165,184.1	487,775.6
	80%	20%	**230**	229,702.4	165,184.1	487,775.6
Belgium	50%	50%	235	326,479.8	165,184.1	487,775.6
	20%	80%	246	423,257.3	165,184.1	487,775.6
	0%	100%	241	487,775.6	165,184.1	487,775.6
	100%	0%	33	3146.6	**3146.6**	**6304.9**
	80%	20%	35	3778.3	3146.7	6305.0
Denmark	50%	50%	36	4725.8	3146.7	6305.0
	20%	80%	36	5673.3	3146.7	6305.0
	0%	100%	33	6305.0	**3146.6**	6305.0
	100%	0%	**423**	126,665.0	126,665.0	**324,734.1**
	80%	20%	469	166,278.8	126,665.0	324,734.2
Chile	50%	50%	460	225,699.6	126,665.0	324,734.2
	20%	80%	472	285,120.3	126,665.0	324,734.2
	0%	100%	485	324,734.1	126,665.0	**324,734.1**

7.2. Vaccination Plan per Problem Instance

In this section, we show for each problem instance its final adjusted curve to their COVID-19 test data. Moreover, the best vaccination plan obtained from previous experiments is applied to the case, the changes between the scenarios with and without vaccination are computed, and the new adjusted curve is displayed.

7.2.1. Austria

Once the adjustment between curves is made for the data of the second wave, the results shown in Figures 4 and 5 of the newly infected per day curve and cumulative cases of the second wave were obtained. The x-axis shows the days since the start of the disease, and the y-axis indicates the number of individuals. It is observed from the newly infected cases that, in the beginning, there is a slow increase, but after 1000 infected per day multiply to the peak, the decay is less abrupt. Moreover, from the cumulative cases near the day of the peak value in both curves, the results are close.

The heuristic algorithm was executed six times with 150 iterations as stopping criteria and 40 iterations with no improvement and the parameter values set in Section 6.2.1. After the execution of the heuristic algorithm proposed, the vaccination plan of 250,000 vaccines per period is obtained. Part of it is shown in Table 7. This table shows the six subgroups to which the higher number of vaccines were allocated.

The first column of the table shows the period of vaccination; all other columns show the subgroups analyzed—in this case, six of the nine states of Austria, including Vienna, Lower Austria, Styria, Tyrol, Salzburg, and Vorarlberg.

It can be observed that in the first two periods, Vorarlberg has a high number of vaccines. This may be due to the fact that at the beginning of the outbreak, this state had more infected individuals than others, and the number of infected did not increase much until the third vaccination. In the fourth and fifth vaccination, Lower Austria and Styria have a high number of vaccines. This can be attributed to how connected these states are to other states.
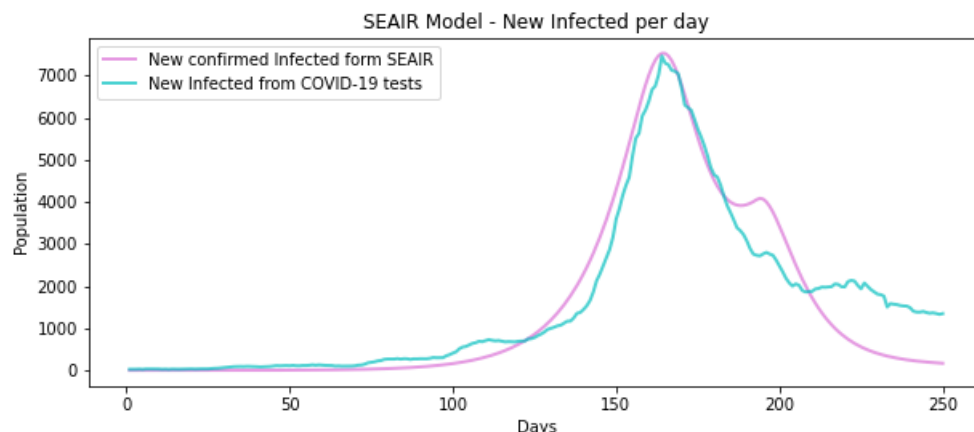
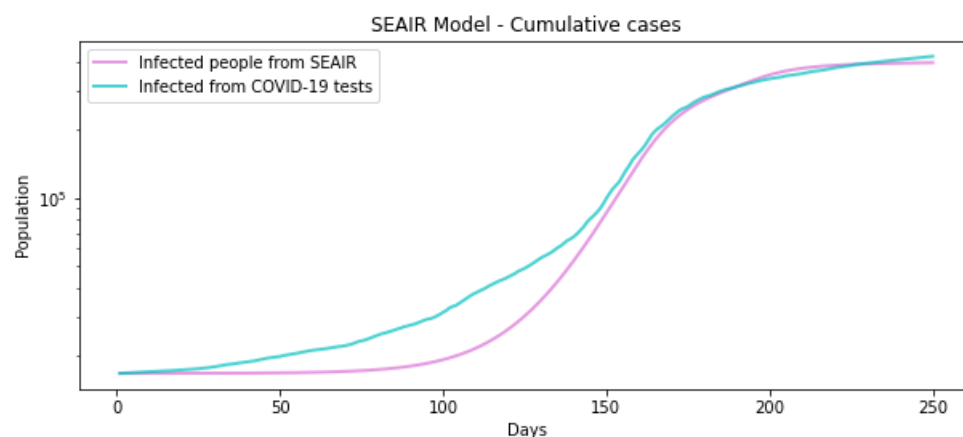**Figure 4.** Comparison of newly infected people between SEAIR model and COVID-19 tests in Austria. Second wave.

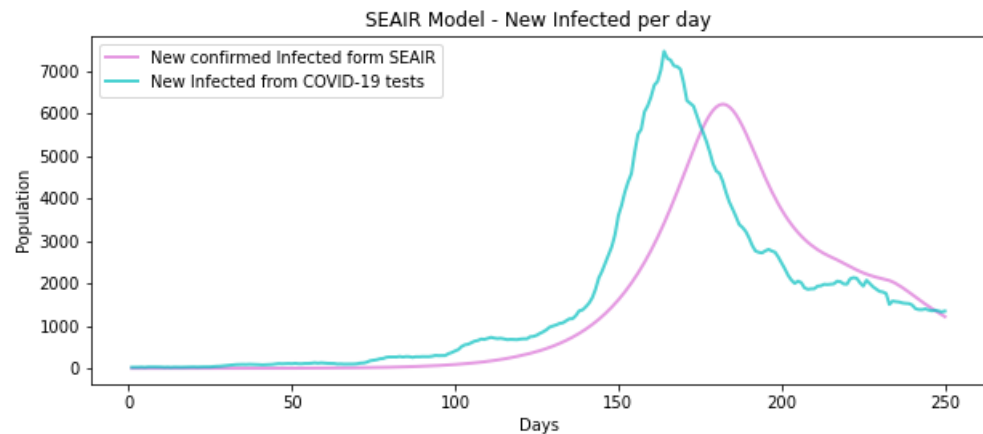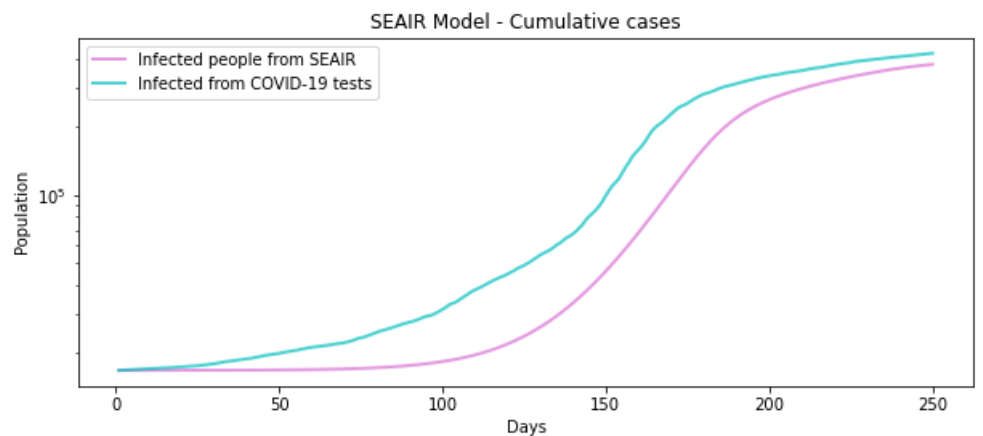**Figure 5.** Comparison of cumulative infected people between SEAIR model and COVID-19 tests in Austria. Second wave.

Table 7. Vaccines corresponding to the most vaccinated subgroups of the best vaccination plan obtained from SEAIRV model.

	Vienna	Lower Austria	Styria	Tyrol	Salzburg	Vorarlberg
1st Vac.	0	0	0	0	0	250,000
2nd Vac.	80,493	4436	767	3231	5138	111,973
3rd Vac.	3040	89,984	48,955	8555	82,470	139
4th Vac.	0	136,992	23,061	51,267	0	0
5th Vac.	0	18,918	132,868	71,411	0	0

The resulting curves after the vaccination process are shown in Figures 6 and 7. Here, the x-axis shows the days, and the y-axis shows the number of individuals. From the newly infected per day curve, it can be observed that the peak decreases from more than 7000 to almost 6000, compared with the previous SEAIR curve without vaccination of Figure 4, which drops to nearly zero on day 250. In this case, the curve decreases slowly after the peak value. Moreover, from the cumulative instances, it is observed that the number of cases increases a bit after day 100 compared to the curve of COVID-19 tests, which starts almost at day 0.

Figure 6. Comparison of cumulative infected people between SEAIR model and COVID-19 tests in Austria's second wave after applying the best vaccination plan found.

Figure 7. Comparison of cumulative infected people between SEAIR model and COVID-19 tests in Austria's second wave after applying the best vaccination plan found.

Figure 8 shows the curves of each of the subgroups in Austria when the best vaccination plan found is applied. In these Figures, the number of susceptible (S), exposed (E), asymptomatic (A), infected (I), and recovered (R), and new infections over time are presented. In all these plots, the x-axis shows the days since the start of the disease, and the y-axis indicates the number of individuals. It can be observed from the exposed, asymptomatic, infected, and newly infected curves how the Voralberg subgroup has its peak after day 200. This is when all the other subgroups have peaks close to day 180. This can be due to the first and second vaccination because it covers more than two-thirds of their populations.

8×10^3 The results of the vaccination plan compared to the nonvaccination plan are shown in Table 8. The first column of the table corresponds to the evaluated criterion: the total infected population, maximum number of infected and asymptomatic at the same time, maximum number of infected at the same time, and maximum number of newly infected individuals per day (or the peak of the curve). The following columns show the corresponding result with the best vaccination plan, without vaccination, and the related perceptual gain. This vaccination plan covers about 13.99% of the total Austrian population, and it is observed that, in this case, the decrease percentages are higher than this value. The whole infected is the value that decreases when vaccination is applied. Regarding the other criterion, they have almost the same decreasing value; this can be attributed to the movement restrictions and the quantity of asymptomatic population of 30% being the lower from all the problem instances.
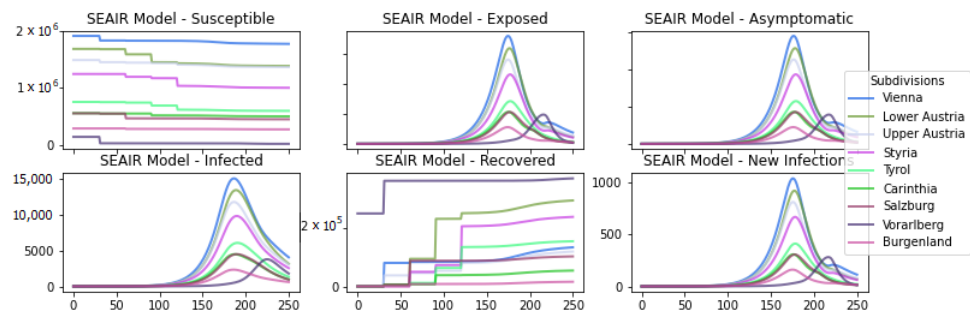
Figure 8. Plots of susceptible, exposed, asymptomatic, infected, recovered, and newly infected individuals per day for each region of the SEAIR model with the best vaccination plan found.

Table 8. Comparison table of infections with and without vaccination.

	With Best Vaccination	Without Vaccination	Decrease Percentage
Total Infected	245,494.840	306,179.115	19.820%
Maximum Infected and Asymptomatic	70,114.634	85,351.480	17.852%
Maximum Infected	68,085.025	82,903.757	17.875%
Maximum Newly Infected per Day	4648.093	5645.949	17.674%

7.2.2. Belgium

Adjustments to the SEAIRV model are shown in Figures 9 and 10. These Figures show the curve of the newly infected per day and cumulative cases of the second wave. From the newly infected cases, it can be observed that the curve has a very marked peak and a similar inclination between the increase in patients until the peak and the decrease of the curve after the peak value. Moreover, the COVID-19 test curve does not end close to zero; rather, it shows an equilibrium state close to 2500 newly infected per day. Regarding the cumulative cases, both curves have a prominent inclination between days 75 and 100.
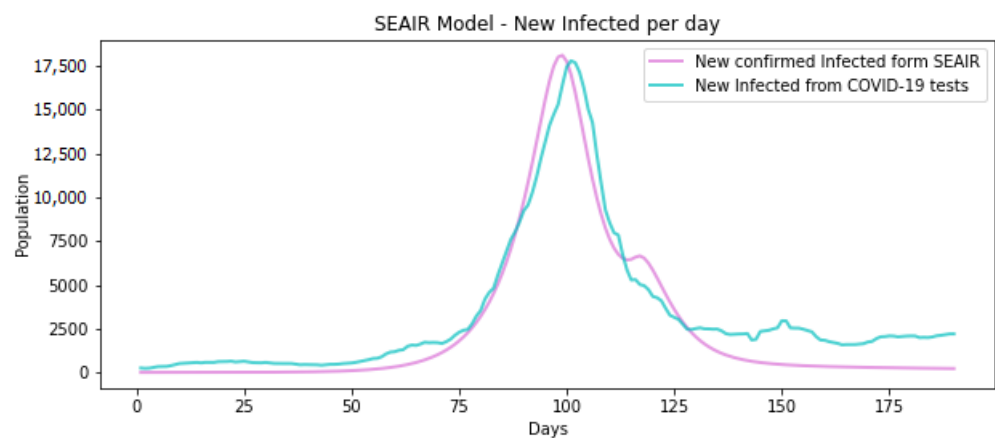
Figure 9. Comparison of newly infected people between SEAIR model and COVID-19 tests in Belgium. Second wave.

From the experiments of the heuristic approach, the vaccination plan of 300,000 vaccines per period was obtained. Part of it is shown in Table 9, which shows the six subgroups to which a higher number of vaccines were allocated. The first column of the table shows

the period of vaccination; all other columns show the subgroups considered. In this case, six of the 11 provinces of Belgium—Flemish Brabant, Antwerp, Liège, Walloon Brabant, Limburg and Namur—were considered.
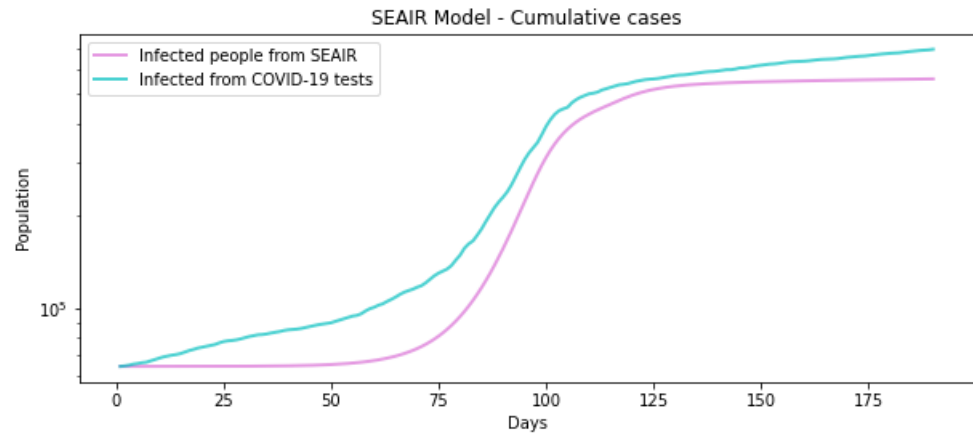
Figure 10. Comparison of cumulative infected people between SEAIR model and COVID-19 tests in Belgium. Second wave.

During the first and fourth vaccination periods, all the vaccines were allocated to Antwerp province, but in the other periods, there were almost no allocations. The first possible reason can be related to the number of infected populations after the vaccination starts decreasing and different subgroups start to have more infected people. Another possible explanation can be connected to the restriction measures. Antwerp province had too many infected populations, and individuals here started decreasing their movement reaching the point that vaccination would little change the spread of the virus.

Table 9. Vaccines corresponding to the most vaccinated subdivision of the best vaccination plan obtained from SEAIRV model.

	Flemish Brabant	Antwerp	Liège	Walloon Brabant	Limburg	Namur
1st Vac.	0	0	300,000	0	0	0
2nd Vac.	91,507	47,449	0	20,133	4935	10,067
3rd Vac.	59,017	29,817	16	13,188	83,452	30,376
4th Vac.	0	0	0	300,000	0	0
5th Vac.	1380	2656	0	62,231	0	225,805

In Figures 11 and 12, the resulting curves after the vaccination plan are displayed. Again, the x-axis shows the days since the start of the disease, and the y-axis indicates the number of individuals. It is observed how the curve of newly infected individuals per day shifts to the right; also, the peak decreases its value, and the decay after the peak is softer and takes longer to get to zero newly infected individuals per day. This is compared to the curve without the vaccination obtained with the SEAIR model. The cumulative cases maintain a similar shape, but the values of the SEAIR model are always lower.

Figure 13 shows the curves of each of the subdivisions in Belgium when the best vaccination plan found is applied. It can be observed that most subgroups' exposed, asymptomatic, and newly infected curves have a similar shape concerning the plot of the first curve without vaccination. However, there are two exceptions. The first one corresponds to Wallon Brabant, from which one can see two waves or two peak values due to vaccination. The other exception is Hainaut, which has a slower, smoother fall from the curve after the peak value that looks more like the infected curve. From the susceptible and

recovered plots, it is observed that vaccinations were varied, distributing different vaccines to different groups in each period.
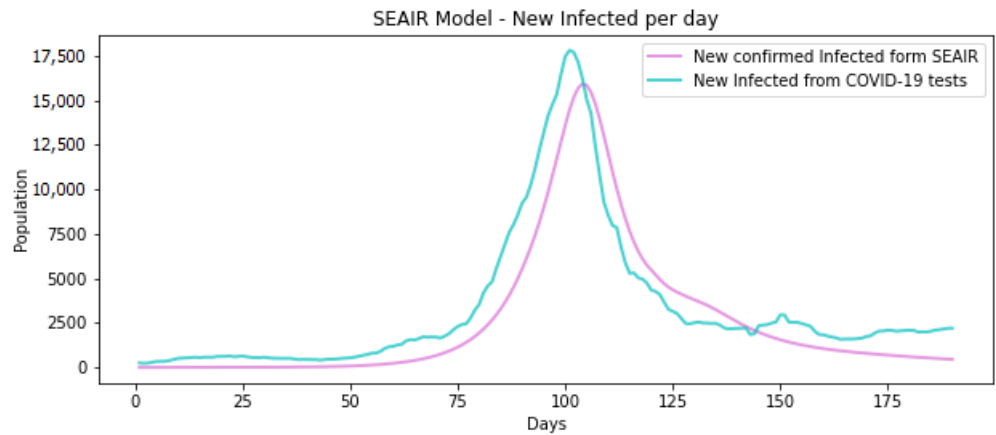

Figure 11. Comparison of cumulative infected people between SEAIR model and COVID-19 tests in Belgium's second wave after applying the best vaccination plan found.
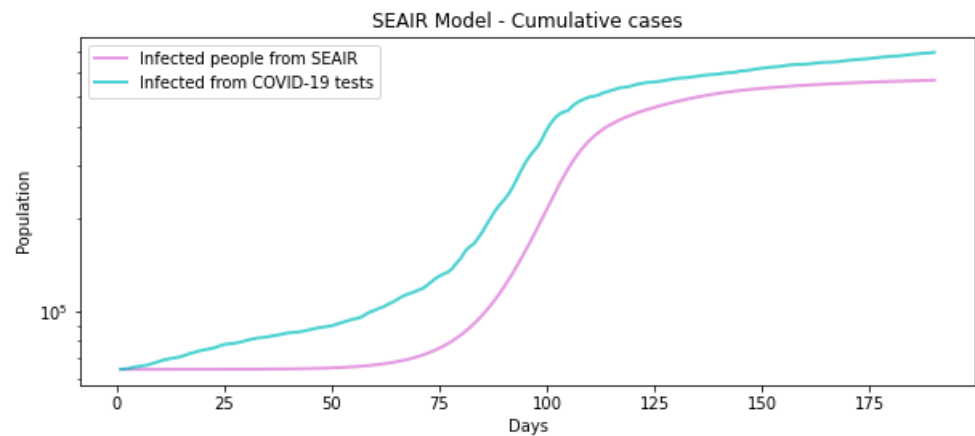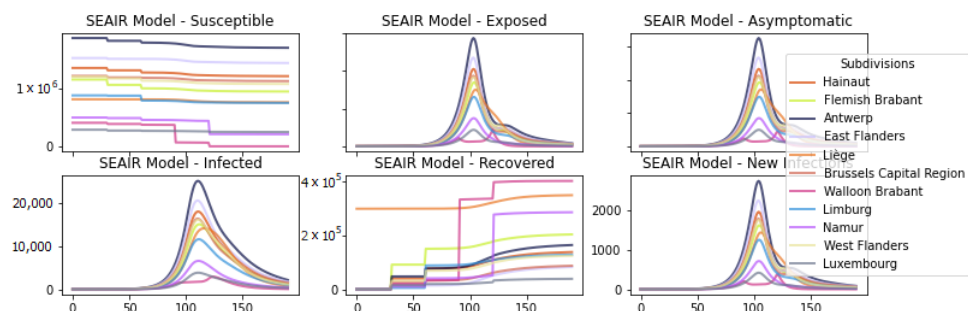

Figure 12. Comparison of cumulative infected people between SEAIR model and COVID-19 tests in Belgium's second wave after applying the best vaccination plan found.

Figure 13. Plots of susceptible, exposed, asymptomatic, infected, recovered, and newly infected individuals per day for each region of the SEAIR model with the best vaccination plan found.

This vaccination plan covers about 13.12% of the total Belgian population, and it is observed that, in this case, the decrease percentages are lower than this value (Table 10). Unlike the other vaccination plans, a slight increase in the total number of infected is obtained here. This can be due to the movement factors of the infected population. This instance has the highest movement factor for the infected people. This can induce a higher value of the infected population to restrict their movement completely. By decreasing the

maximum number of newly infected per day, more freedom to move to the infected people can be allowed.

Table 10. Comparison table of infections with and without vaccination.

	With Best Vaccination	Without Vaccination	Decrease Percentage
Total Infected	502,679.096	495,482.655	−1.452%
Maximum Infected and Asymptomatic	155,287.904	169,063.317	8.148%
Maximum Infected	148,644.350	161,669.909	8.057%
Maximum Newly Infected per Day	15,914.796	18,116.113	12.151%

7.2.3. Denmark

To apply the SEAIRV model, Figures 14 and 15 show the curve of newly infected per day and cumulative cases of the second wave. The x-axis shows the days since the start of the disease, and the y-axis indicates the number of individuals. It can be observed that the peak of the newly infected individuals per day curves is almost the same; also, after the peak, there is a decrease of both curves to a comparable value. For the cumulative cases, the curves get close and show a moderate slope between days 100 and 200.
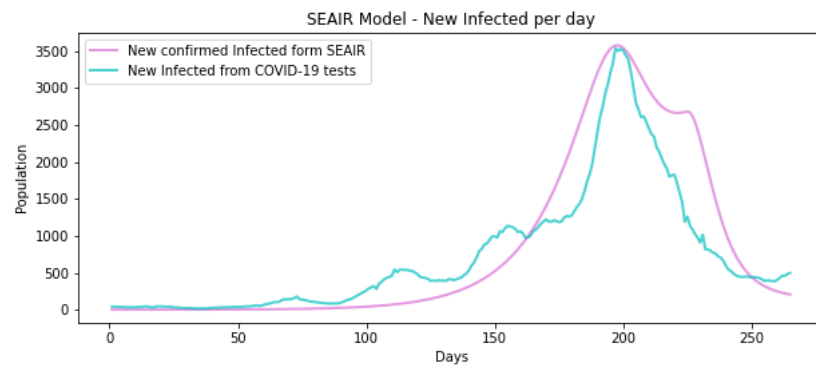
Figure 14. Comparison of newly infected people between SEAIR model and COVID-19 tests in Denmark's second wave.
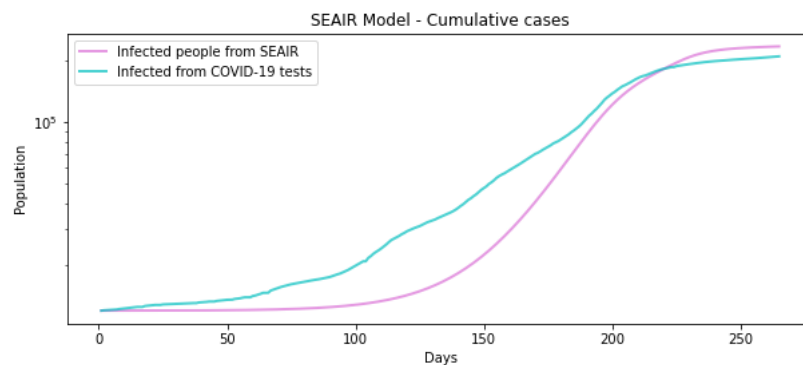
Figure 15. Comparison of cumulative infected people between SEAIR model and COVID-19 tests in Denmark's second wave.

Once it has been verified that the curves are similar, it is possible to execute the algorithm, in this case, with the goal to vaccinate 250,000 people every 30 days five times, or vaccinate until day 150. The best-obtained vaccination plan is shown in Table 11.

The first column of the table corresponds to the period of vaccination. The following columns correspond to the subgroup's name. In this case, Hovedstaden, Midtjylland, Syddanmark, Sjælland, and Nordjylland are the five regions of Denmark.

Table 11. Best vaccination plan obtained from SEAIRV model.

	Hovedstaden	Midtjylland	Syddanmark	Sjælland	Nordjylland
1st Vac.	0	0	0	0	250,000
2nd Vac.	168,060	56,363	419	25,158	0
3rd Vac.	14,360	0	196,157	39,483	0
4th Vac.	179,988	15,631	32,347	22,034	0
5th Vac.	13,176	124,383	41,548	70,893	0

The first vaccination allocates all the vaccines to the subgroup that starts with the infected population. For this case, the problem instance has the lowest basic reproduction number (R_0), implying that the virus spreads more slowly than in the other cases. At the beginning of the first period, between days 0 and 30, the infected population started in Nordjylland and, because of the instance characteristics, did not spread enough to other subgroups. The distribution is more varied for the other vaccination periods; this is because the infected population starts spreading faster and is influenced by the contact between subgroups. In addition, it is observed that Hovedstaden is the one that gets more total vaccines; this is probably because it is the subgroup with a larger population.

In Figures 16 and 17, the resulting curves after the vaccination plan are displayed. Again, the x-axis shows the days since the start of the disease, and the y-axis indicates the number of individuals. It is observed how the curve of newly infected per day is now much flatter and grows more slowly, generating a shift in the position of the peak. Furthermore, in the curve of the cumulative case, it is noticed how the maximum quantity of infected decrease with vaccination and also how the slope has a lower inclination.

In Figure 18, the curves of each of the subgroups in Denmark after the best vaccination plan found by the SEAIRV algorithm is applied are displayed. It can be observed from the susceptible population that the vaccination does not follow a similar pattern in time. Moreover, for three of the five regions—Hovedstaden, Syddanmark, and Sjælland—vaccines are granted for four periods consecutively. Moreover, the second region with less population (Midtjylland) obtains fewer recovered people. This may be because this area is not a region that is too infectious and does not infect other areas.
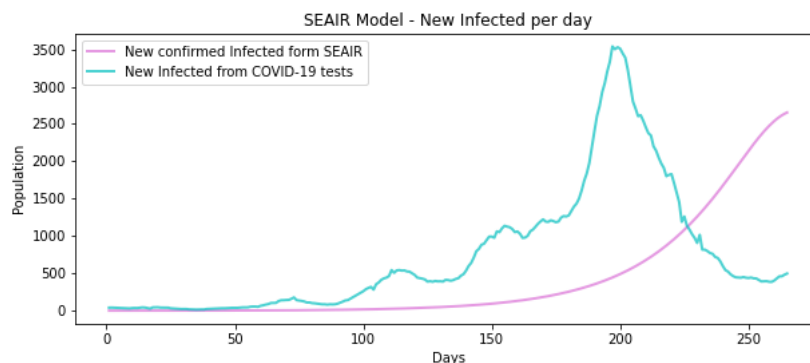

Figure 16. Comparison of cumulative infected people between SEAIR model and COVID-19 tests in Denmark's second wave after applying the best vaccination plan found.
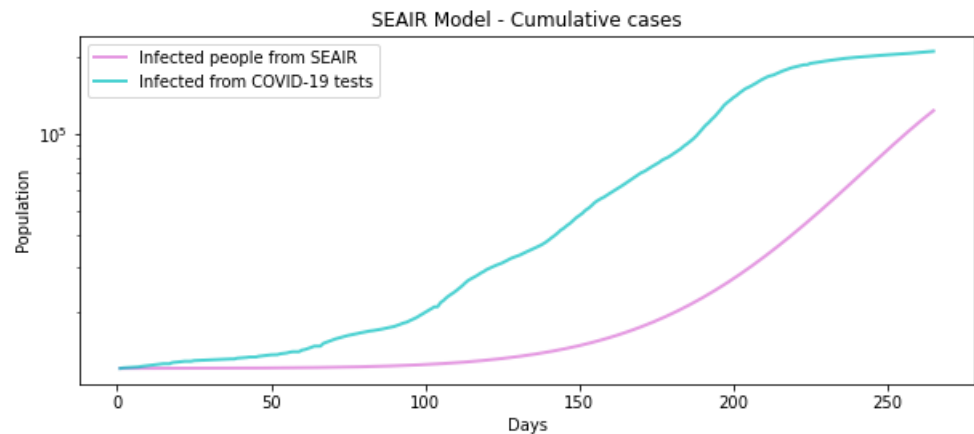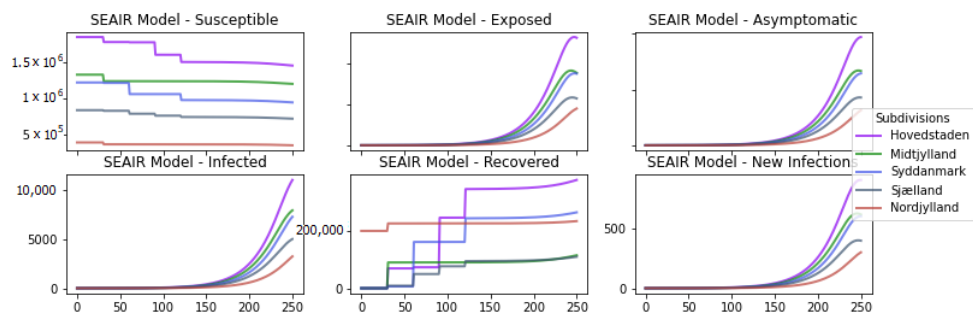
Figure 17. Comparison of cumulative infected people between SEAIR model and COVID-19 tests in Denmark's second wave after applying the best vaccination plan found.

Figure 18. Plots of susceptible, exposed, asymptomatic, infected, recovered, and newly infected individuals per day for each region of the SEAIR model with the best vaccination plan found.

The comparison between values obtained with and without vaccination is shown in Table 12. The first column of the table corresponds to the evaluated criterion, which can be the total infected population, the maximum quantity of infected and asymptomatic at the same time, the maximum amount of infected at the same time, and the maximum newly infected individuals per day (or the peak of the curve). The following columns show the corresponding results with the best vaccination applied and without vaccination. The last column shows the improvement percentage after the vaccination plan is used.

Table 12. Comparison table of infections with and without vaccination.

	With Best Vaccination	Without Vaccination	Decrease Percentage
Total Infected	74,113.695	218,113.191	66.021%
Maximum Infected and Asymptomatic	26,976.820	49,953.341	45.996%
Maximum Infected	22,582.891	43,118.680	47.626%
Maximum Newly Infected per Day	2141.13	3577.559	40.151%

In this case, the total number of vaccines applied at the end of the period corresponds to 21.40% of the population. A decreasing percentage from the total infected of 66.021% was obtained. This high value can be due to the fact that after vaccination, the curve

flattens and reaches its peak value in many more days. The maximum number of infected, asymptomatic, and newly infected individuals per day decreased similarly.

7.2.4. Chile

For Chile, the model was adjusted to fit both its first and second waves. The curve of newly infected individuals per day after these adjustments is presented in Figure 19, and the cumulative infected population is in Figure 20. For both graphs, the x-axis shows the period (days), and the y-axis indicates the number of individuals. For this case, a vacation period was applied from day 310 to 370 with an increase in the movement of infected and noninfected population of 0.001. From the newly infected curve, it can be seen that the peak occurs approximately on day 110; the COVID-19 data curve gets an equilibrium state from day 150 to 300 of approximately 2000 people per day. The SEAIR model curve reaches its equilibrium at about 3000 people per day. The cumulative cases after day 100 from both curve values are similar until day 350.
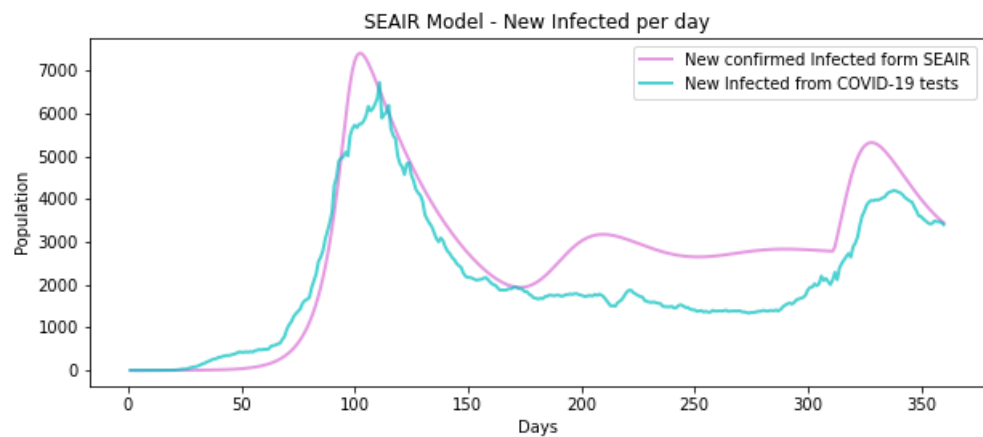

Figure 19. Comparison of newly infected people between SEAIR Model and COVID-19 tests in Chile. First and second wave.
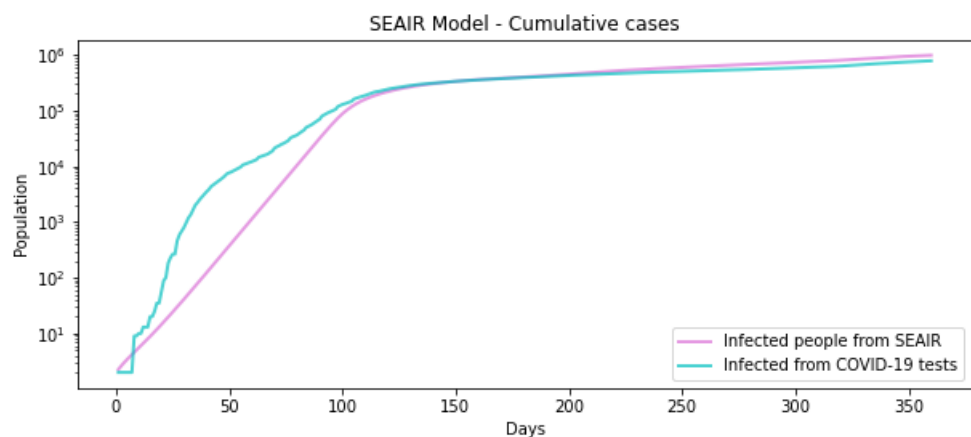

Figure 20. Comparison of cumulative infected people between SEAIR model and COVID-19 tests in Chile. First and second wave.

The solution for the vaccination plan of 500,000 vaccines per period was obtained. Part of it is shown in Table 13. This table shows the six subgroups to which a higher number of vaccines were allocated. The first column of the table shows the period of vaccination; all other columns show the subgroups considered. In this case, six of the 11 regions of Chile are shown: Metropolitan, Bíobío, Los Lagos, Ñuble, Los Ríos, and Arica y Parinacota. It can be seen that the metropolitan region and Los Lagos are the subgroups that have more vaccines allocated. The metropolitan region is the subgroup with greater population and is

the most connected. The Los Lagos region is where the infectious cases started. With regard to the virus's infectiousness, it was slow in the beginning, and during the first 30 days it remained with the subgroup with the more highly infected population.

Table 13. Vaccines corresponding to the most vaccinated subdivision of the best vaccination plan obtained from SEAIRV model.

	Metropolitan	Biobío	Los Lagos	Ñuble	Los Ríos	Arica y Parinacota
1st Vac.	0	0	500,000	0	0	0
2nd Vac.	292,324	65,504	537	186	2084	113
3rd Vac.	410,403	0	0	0	0	0
4th Vac.	0	52,199	33,2241	94,743	0	0
5th Vac.	0	0	0	32,033	374,274	93,397

The resulting curve after the vaccination process is shown in Figures 21 and 22. Here, the x-axis shows the days, and the y-axis shows the number of individuals. It is observed from the newly infected per day that the peak value slightly decreases, and the curve shifts moderately to the right side. From the cumulative cases, a modest decrease can be observed.
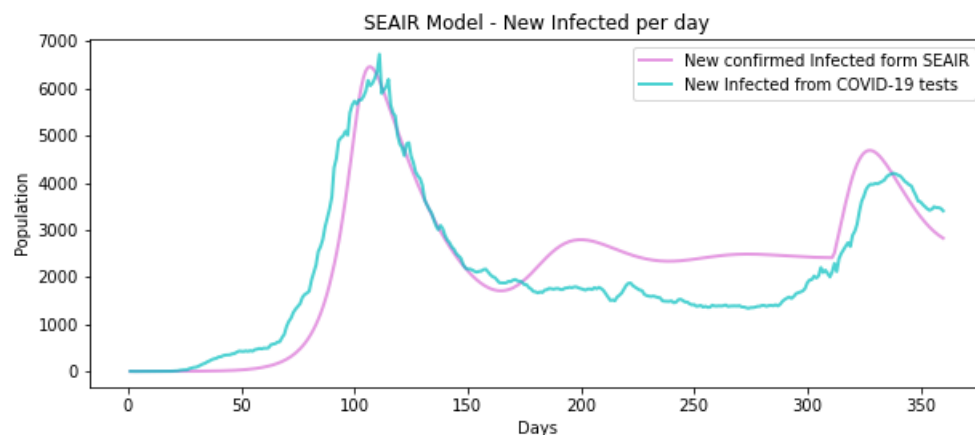

Figure 21. Comparison of cumulative infected people between SEAIR model and COVID-19 tests in Chile's second wave after applying the best vaccination plan found.
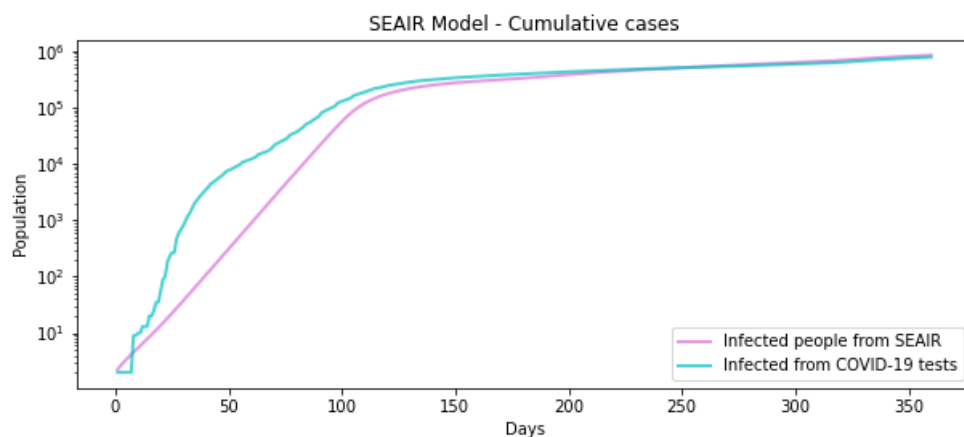

Figure 22. Comparison of cumulative infected people between the SEAIR model and COVID-19 tests in Chile's second wave after applying the best vaccination plan found.

Figure 23 shows the curves of each of the subdivisions in Chile when the best vaccination plan found was applied. The big difference between the population of the metropolitan region and other subgroups can be seen. Furthermore, the difference between the shape of the asymptomatic and infected curves, where differences between the peak and the state of equilibrium are much more pronounced in the asymptomatic curve, can be seen. This is due to the freedom of movement that the asymptomatic population has.
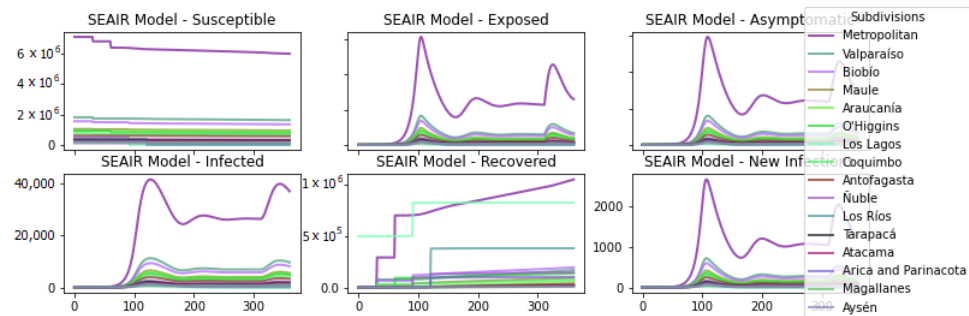

Figure 23. Susceptible, exposed, asymptomatic, infected, recovered, and newly infected individuals per day for each region of the SEAIR model with the best vaccination plan found.

The results of the vaccination plan compared to nonvaccination are shown in Table 14. The first column of the table corresponds to the evaluated criterion: the total infected population, maximum number of infected and asymptomatic at the same time, maximum number of infected at the same time, and maximum number of new infected per day (or the peak of the curve). The next columns show the corresponding results with the best vaccination plan, without vaccination, and the related perceptual gain.

This vaccination plan covers about 14.23% of the total Chilean population, and it is observed that, in this case, the decrease percentages are similar to this value. Unlike the previous problem instances, the difference between the decreased percentage of total infected and maximum infected is unimportant. It should be emphasized that, for this problem, different parameter configurations showed better performance, so it is highly possible that there were much better vaccination plans that delivered a better value for these types of problems.

Table 14. Comparison table of infections with and without vaccination.

	With Best Vaccination	Without Vaccination	Decrease Percentage
Total Infected	840,096.735	983,040.848	14.541%
Maximum Infected and Asymptomatic	111,306.477	129,594.850	14.112%
Maximum Infected	101,152.092	117,983.213	14.266%
Maximum Newly Infected per Day	6465.033	7410.361	12.757%

8. Conclusions

In this work, we studied and modeled the COVID-19 spread through subgroups that were as close as possible to the observed, measured behavior. This mainly considers geographic divisions and interactions with the idea of finding efficient vaccination plans considering intervals of periods where vaccines are available. It also considers decreasing the maximum number of infected people at the same time and the total infected population of the obtained model.

The adjustments to get closer to each COVID-19 test curve were based on COVID-19 and SEAIR parameters that determine the restriction movement for infected and noninfected populations. We sought to assimilate, as much as possible, the peak of the newly infected curve, the day of the peak, the inclination in the cumulative case curve, and the shape of the fall after the curve.

Two types of experiments were performed. The first ones were oriented to analyze the SEAIRV parameter values, and the second ones were oriented to get the vaccination plans for each problem. From the first experiments, it was possible to conclude that the best parameter values for the SEAIRV algorithm were the All to One initialization due to the lower time obtained with it with presumed faster convergence and stagnation. Probabilities of 80%, 10% and 10% existed for the movements Give Random, Swap Random, and Invert Random, respectively. There is a big necessity for the Give Random movement, which changes the proportion of the number of vaccines per subgroup, and the other two movements can support a faster convergence. Finally, the distribution of half of the importance to each objective function is low because of the time taken to converge and search for solutions with both objectives.

Another of the conclusions obtained from these experiments was that there are problematic instances with opposite objectives; for example, there are solutions with a more infected population at the same time but a lower value of total infected individuals in the period.

For the proposed method, when looking for the combination of vaccines per period and taking into account that period and not future ones, the first population infected in most of the cases influences the allocation of vaccines to these subgroups. Furthermore, it has been shown that despite the percentage of the population vaccinated with small portions, it is possible to make more significant changes depending on the vaccination plan, the reproduction number, and the movements of the infected and noninfected population.

In future work, some additional scenarios can be studied, e.g. the use of real movement data between subdivisions to get problem instances closer to reality. In addition, we can add more subgroups with different ages and prioritize vaccinating some of them or seeing that they have other movement or contact. We can change the way to find vaccines per period, focusing on the time after the last vaccination to see if we can find better combinations. We can find new movements to allow a faster convergence to high-quality solutions.

Author Contributions: Conceptualization, C.H.-V. and E.M.; investigation, C.H.-V. and E.M.; methodology, C.H.-V. and E.M.; software, C.H.-V.; supervision, E.M.; validation, C.H.-V. and E.M.; writing—original draft, C.H.-V.; writing—review and editing, E.M. All authors have read and agreed to the published version of the manuscript.

Institutional Review Board Statement: Not applicable.

Informed Consent Statement: Not applicable.

Data Availability Statement: Problem instances are available in the specified website.

Conflicts of Interest: The authors declare no conflict of interest.

References

1. Liu, Y.C.; Kuo, R.L.; Shih, S.R. COVID-19: The first documented coronavirus pandemic in history. *Biomed. J.* **2020**, *43*, 328–333. [CrossRef] [PubMed]
2. Cucinotta, D.; Vanelli, M. WHO Declares COVID-19 a Pandemic. *Acta Bio Med.* **2020**, *91*, 157. [CrossRef]
3. Ke, R.; Sanche, S.; Romero-Severson, E.; Hengartner, N. Fast spread of COVID-19 in Europe and the US suggests the necessity of early, strong and comprehensive interventions. *medRxiv* **2020**. [CrossRef]
4. Knox, L.; Karantzas, G.C.; Romano, D.; Feeney, J.A.; Simpson, J.A. One year on: What we have learned about the psychological effects of COVID-19 social restrictions: A meta-analysis. *Curr. Opin. Psychol.* **2022**, *46*, 101315. [CrossRef] [PubMed]
5. Costa-Font, J.; Vilaplana-Prieto, C. Risky restrictions? Mobility restriction effects on risk awareness and anxiety. *Health Policy* **2022**, *126*, 1090–1102. [CrossRef]

6.   Chen, Y.T. Effect of vaccination patterns and vaccination rates on the spread and mortality of the COVID-19 pandemic. *Health Policy Technol.* **2022**, 100699. [CrossRef] [PubMed]

7.   Goldstein, J.R.; Cassidy, T.; Wachter, K.W. Vaccinating the oldest against COVID-19 saves both the most lives and most years of life. *Proc. Natl. Acad. Sci. USA* **2021**, *118*, e2026322118. [CrossRef]

8.   Rimmelzwaan, G.F.; Bodewes, R.; Osterhaus, A.D. Vaccination strategies to protect children against seasonal and pandemic influenza. *Vaccine* **2011**, *29*, 7551–7553. [CrossRef]

9.   Gu, S.; Jiang, M.; Guzzi, P.H.; Milenković, T. Modeling multi-scale data via a network of networks. *Bioinformatics* **2022**, *38*, 2544–2553. [CrossRef]

10. Keeling, M.J.; Eames, K.T. Networks and epidemic models. *J. R. Soc. Interface* **2005**, *2*, 295–307. [CrossRef]

11. Petrizzelli, F.; Guzzi, P.H.; Mazza, T. Beyond COVID-19 pandemic: Topology-aware optimization of vaccination strategy for minimizing virus spreading. *Comput. Struct. Biotechnol. J.* **2022**, *20*, 2664–2671. [CrossRef] [PubMed]

12. Varotsos, C.A.; Krapivin, V.F.; Xue, Y.; Soldatov, V.; Voronova, T. COVID-19 pandemic decision support system for a population defense strategy and vaccination effectiveness. *Saf. Sci.* **2021**, *142*, 105370. [CrossRef] [PubMed]

13. Schneckenreither, G.; Popper, N.; Zauner, G.; Breitenecker, F. Modelling SIR-type epidemics by ODEs, PDEs, difference equations and cellular automata—A comparative study. *Simul. Model. Pract. Theory* **2008**, *16*, 1014–1023. [CrossRef]

14. Bacaër, N. McKendrick and Kermack on epidemic modelling (1926–1927). In *A Short History of Mathematical Population Dynamics*; Springer: London, UK, 2011; pp. 89–96. [CrossRef]

15. Li, M.Y.; Muldowney, J.S. Global stability for the SEIR model in epidemiology. *Math. Biosci.* **1995**, *125*, 155–164. [CrossRef] [PubMed]

16. Maltz, A.; Fabricius, G. SIR model with local and global infective contacts: A deterministic approach and applications. *Theor. Popul. Biol.* **2016**, *112*, 70–79. [CrossRef]

17. Fabricius, G.; Maltz, A. Exploring the threshold of epidemic spreading for a stochastic SIR model with local and global contacts. *Phys. A Stat. Mech. Its Appl.* **2020**, *540*, 123208. [CrossRef]

18. Fu, L.; Song, W.; Lv, W.; Lo, S. Simulation of emotional contagion using modified SIR model: A cellular automaton approach. *Phys. A Stat. Mech. Its Appl.* **2014**, *405*, 380–391. [CrossRef]

19. Tanner, M.W.; Sattenspiel, L.; Ntaimo, L. Finding optimal vaccination strategies under parameter uncertainty using stochastic programming. *Math. Biosci.* **2008**, *215*, 144–151. [CrossRef]

20. Chen, S.; Small, M.; Fu, X. Global stability of epidemic models with imperfect vaccination and quarantine on scale-free networks. *IEEE Trans. Netw. Sci. Eng.* **2019**, *7*, 1583–1596. [CrossRef]

21. Correa Cordova, M.L.; Geletu, A.; Li, P. Optimal Scheduling of Vaccination Campaigns Using a Direct Dynamic Optimization Method. *IFAC-PapersOnLine* **2016**, *49*, 207–212. [CrossRef]

22. Wu, Q.; Lou, Y. Local immunization program for susceptible-infected-recovered network epidemic model. *Chaos Interdiscip. J. Nonlinear Sci.* **2016**, *26*, 023108, [CrossRef] [PubMed]

23. da Cruz, A.R.; Cardoso, R.T.; Takahashi, R.H. Multiobjective synthesis of robust vaccination policies. *Appl. Soft Comput.* **2017**, *50*, 34–47. [CrossRef]

24. Kim, D.; Guo, H.; Wang, W.; Lee, J.L.; Kwon, S.S.; Tokuta, A.O. On efficient vaccine distribution strategy to suppress pandemic using social relation. *Discret. Math. Algorithms Appl.* **2016**, *8*, 1650010. [CrossRef]

25. Wang, X.; Peng, H.; Shi, B.; Jiang, D.; Zhang, S.; Chen, B. Optimal vaccination strategy of a constrained time-varying SEIR epidemic model. *Commun. Nonlinear Sci. Numer. Simul.* **2019**, *67*, 37–48. [CrossRef]

26. Ng, C.; Cheng, T.C.E.; Tsadikovich, D.; Levner, E.; Elalouf, A.; Hovav, S. A multi-criterion approach to optimal vaccination planning: Method and solution. *Comput. Ind. Eng.* **2018**, *126*, 637–649. [CrossRef]

27. Halloran, M.; Struchiner, C.; Longini, I. Study Designs for Evaluating Different Efficacy and Effectiveness Aspects of Vaccines. *Am. J. Epidemiol.* **1997**, *146*, 789–803. [CrossRef]

28. Enayati, S.; Özaltin, O.Y. Optimal influenza vaccine distribution with equity. *Eur. J. Oper. Res.* **2020**, *283*, 714–725. [CrossRef]

29. Glover, F.; Laguna, M. Tabu Search. In *Handbook of Combinatorial Optimization: Volume1–3*; Du, D.Z., Pardalos, P.M., Eds.; Springer: Boston, MA, USA, 1998; pp. 2093–2229. [CrossRef]

30. Liang, L.Y.; Chao, W.C. The strategies of tabu search technique for facility layout optimization. *Autom. Constr.* **2008**, *17*, 657–669. [CrossRef]

31. Euchi, J. The vehicle routing problem with private fleet and multiple common carriers: Solution with hybrid metaheuristic algorithm. *Veh. Commun.* **2017**, *9*, 97–108. [CrossRef]

32. Global Change Data Lab. Ourworldindata. Available online: https://www.nasa.gov/nh/pluto-the-other-red-planet (accessed on 10 March 2021).

33. DATA UC. Visualizador Covid-19 Chile. Available online: https://coronavirus.mat.uc.cl/ (accessed on 10 March 2021).

34. Gao, Y. Treewidth of Erdös–Rényi random graphs, random intersection graphs, and scale-free random graphs. *Discret. Appl. Math.* **2012**, *160*, 566–578. [CrossRef]

35. Volchenkov, D.; Blanchard, P. An algorithm generating random graphs with power law degree distributions. *Phys. A Stat. Mech. Its Appl.* **2002**, *315*, 677–690. [CrossRef]

36. Vega Yon, G.G.; Slaughter, A.; de la Haye, K. Exponential random graph models for little networks. *Soc. Netw.* **2021**, *64*, 225–238. [CrossRef]

37. National Center for Immunization and Respiratory Diseases. CDC Coronavirus Planning Scenarios. Available online: www.cdc.gov/coronavirus/2019-ncov/hcp/planning-scenarios.html (accessed on 10 March 2021).

38. Heneghan, C.; Brassey, J.; Jefferson, T. CEBM Portion of Asymptomatic of COVID-19. Available online: http://www.cebm.net/covid-19/covid-19-what-proportion-are-asymptomatic/ (accessed on 10 March 2021).